Astronomy & Astrophysics

Variable stars in the VVV globular clusters

III. RR Lyrae stars in the inner Galactic globular clusters

Javier Alonso-García[1,2,*], Leigh C. Smith[3], Jason L. Sanders[4], Dante Minniti[5,6], Márcio Catelan[7,2],
Gonzalo Aravena Rojas[8,9], Julio A. Carballo-Bello[10], José G. Fernández-Trincado[11], Carlos E. Ferreira Lopes[12,2],
Elisa R. Garro[13], Zhen Guo[8,2,14], Maren Hempel[5,15], Philip W. Lucas[14], Daniel Majaess[16],
Roberto K. Saito[17], and A. Katherina Vivas[18]

(Affiliations can be found after the references)

ABSTRACT

Context. High reddening near the Galactic plane hampers observations and proper characterization of the globular clusters (GCs) located toward the inner regions of the Milky Way.

Aims. The VISTA Variables in the Vía Láctea (VVV) survey observed the Galactic bulge and adjacent disk for several years, providing multi-epoch, near-infrared images for 41 Galactic GCs. Detecting RR Lyrae variable stars belonging to these GCs will aid in their accurate parameterization.

Methods. By fully leveraging the astrometric, photometric, and variability VVV catalogs, we searched for RR Lyrae stars associated with GCs. Our selection criteria, based on proper motions, proximity to the cluster centers, and distances inferred from their period-luminosity-metallicity relations, enable us to accurately identify the RR Lyrae population in these GCs and determine color excesses and distances to these poorly studied GCs in a homogeneous manner. Since the VVV catalogs cover from the innermost regions of the GCs to their outskirts, we can provide a comprehensive picture of the entire RR Lyrae population in these GCs.

Results. We have discovered significant RR Lyrae populations in two highly reddened Galactic GCs: UKS 1 and VVV-CL160, previously unknown to host RR Lyrae stars. Additionally, we have detected one RR Lyrae candidate in each of Terzan 4 and Terzan 9, also new to RR Lyrae detection. We further confirm and increase the number of RR Lyrae stars detected in 22 other low-latitude Galactic GCs. The RR Lyrae distances place most of these GCs within the Galactic bulge, aligning well with the few GCs in our sample with reliable *Gaia* or *Hubble* Space Telescope measurements. However, most of the VVV GCs lack accurate *Gaia* distances, and literature distances are generally significantly smaller than those derived in this work. As a byproduct of our analysis, we have obtained the proper motions for all the VVV GCs, independently confirming *Gaia* results, except for two of the most reddened GCs: UKS 1 and 2MASS-GC02.

Key words. stars: variables: RR Lyrae – globular clusters: general – globular clusters: individual: UKS 1 – globular clusters: individual: VVV-CL160

1. Introduction

The Galactic globular clusters (GCs) constitute some of the most massive and outstanding stellar aggregates in the Milky Way. Their location in the Milky Way allows us to explore in detail their stellar populations, as we can separate their individual stars down to a limit not available for their counterparts in other galaxies. Recent photometric and spectroscopic studies of their member stars from the ground and from space (e.g., Milone et al. 2017; Marino et al. 2019; Baumgardt et al. 2023) have led to a deeper understanding of the nature of these objects. The advent of the *Gaia* mission (Gaia Collaboration 2016) has been a crucial landmark, not only in more accurately establishing the physical parameters of the Galactic GCs (Baumgardt et al. 2019; Vasiliev & Baumgardt 2021), but also for better understanding their origin (Massari et al. 2019; Belokurov & Kravtsov 2024).

However, the GCs located closer to the Galactic plane suffer the effects of high extinction, which prevents their proper characterization when we use optical wavelengths. Near-infrared observations are better suited, as extinction is highly diminished at these wavelengths. Nevertheless, other additional problems present in these regions, such as the elevated density of field

stars, further hamper the study of these GCs. In order to improve our analyses, we need to complement the usual photometric studies of the color-magnitude diagram (CMD) with other tools.

Paramount among them is the search for intrinsically bright pulsating stars such as RR Lyrae variables, which not only provide hints about the old ages of the GCs but can also allow us to precisely measure observational parameters such as distances and reddenings (Catelan & Smith 2015). Near-infrared time-series observations allow us not only to more easily detect these stars despite the high extinction of these low-latitude regions but to more precisely provide the parameters of the GCs by using the tighter period-luminosity-metallicity (PLZ) relations at these wavelengths (e.g., Catelan et al. 2004; Braga et al. 2019; Cusano et al. 2021).

The VISTA Variables in the Vía Láctea survey (VVV; Minniti et al. 2010) provides multi-epoch near-infrared observations of the Galactic bulge and disk, essential for identifying and characterizing the variable stellar populations of the GCs located toward these regions. Approximately one-quarter of the known GCs in the Milky Way are located inside the footprint of the VVV survey. In Alonso-García et al. (2015) and Alonso-García et al. (2021), hereafter referred to as Paper I and Paper II, respectively, we searched for variable stars in

seven low-latitude GCs with different metallicities, presenting our detection algorithm and refining the parametrization of the PLZ relations for the near-infrared filters in the VVV survey. In the current paper, the third in the series, we aim to take full advantage of recent photometric catalogs produced with the VVV data to further investigate the RR Lyrae pulsating stellar populations in the low-latitude GCs within the VVV footprint and use them to better characterize the entire sample of these GCs.

2. Observations and datasets

The VVV survey (Minniti et al. 2010; Saito et al. 2012) used the 4.1 m VISTA telescope at Cerro Paranal Observatory to obtain photometric observations of the Galactic bulge ($-10°.0 \leq l \leq +10°.4$, $-10°.3 \leq b \leq +5°.1$) and an adjacent disk area ($294°.7 \leq l \leq 350°.0$, $-2°.25 \leq b \leq +2°.25$) of the Milky Way in the Z, Y, J, H, and K_s near-infrared filters. The camera on board the VISTA telescope provided 1.5×1.1 deg^2 wide-field images with a resolution of $0.34''$per pixel. The K_s multi-epoch observations from the VVV survey allow for the inspection of photometric variability among the detected sources.

As we detail in the following sections, we use the VVV Infrared Astrometric Catalogue 2 (VIRAC2) and VIrac VAriable Classification Ensemble (VIVACE) databases to carry out such a variability search and characterization in the VVV GCs. The VIRAC2 catalog (Smith et al. 2025), an updated version of the VIRAC database (Smith et al. 2018) now built using point spread function (PSF) photometry, provides positions, proper motions, mean magnitudes, and light curves for all detections from the VVV observations. VIRAC2 uses the DoPHOT software (Schechter et al. 1993; Alonso-García et al. 2012) to detect sources and extract their PSF photometry from the VVV images (Alonso-García et al. 2018) in the different filters and epochs. VIRAC2 extends the timeline of the original VVV observations by incorporating the additional J, H and K_s images taken of these regions in the more recent VVV extended survey (VVVX, Minniti 2018; Saito et al. 2024). Each VVV field used in this work was observed at least twice in Z, Y, J, and H, and at least 70 times in the K_s filter. Photometry from the different sources is later cross-matched and calibrated into the VISTA photometric system (Gonzalez et al. 2018) to produce the multi-epoch near-infrared light curves that were used by VIVACE for detecting variable sources. The VIVACE database (Molnar et al. 2022) is a catalog of variable sources which, using machine-learning techniques, identifies, classifies, and parameterizes variable stars in the VVV original footprint. It uses the VIRAC2 catalog and light curves as input for its variability detections, yielding a catalog of ~1.4 million variable stars, for which it provides, among other parameters, position, variable types, periods, amplitudes, and mean magnitudes in the different VVV near-infrared filters.

3. Analysis

The VIVACE catalog already provides a list of variable sources in the region of the VVV GCs. A comparison with the seven GCs sampled in Paper II reveals that nearly all of the RR Lyrae stars reported there are also present in the VIVACE catalog. In addition to other light curve parameters, VIVACE provides precise periods for the RR Lyrae stars, enabling the construction of phased light curves from our VIRAC2 photometry, of the same quality as those presented in Paper II. VIVACE also offers

sub-classifications for the RR Lyrae stars, distinguishing between fundamental-mode (RRab) and first-overtone (RRc) types. Thus, we decided not to further search for more RR Lyrae variable stars in the remaining VVV GCs and instead to inspect all the VIVACE detections in their surroundings.
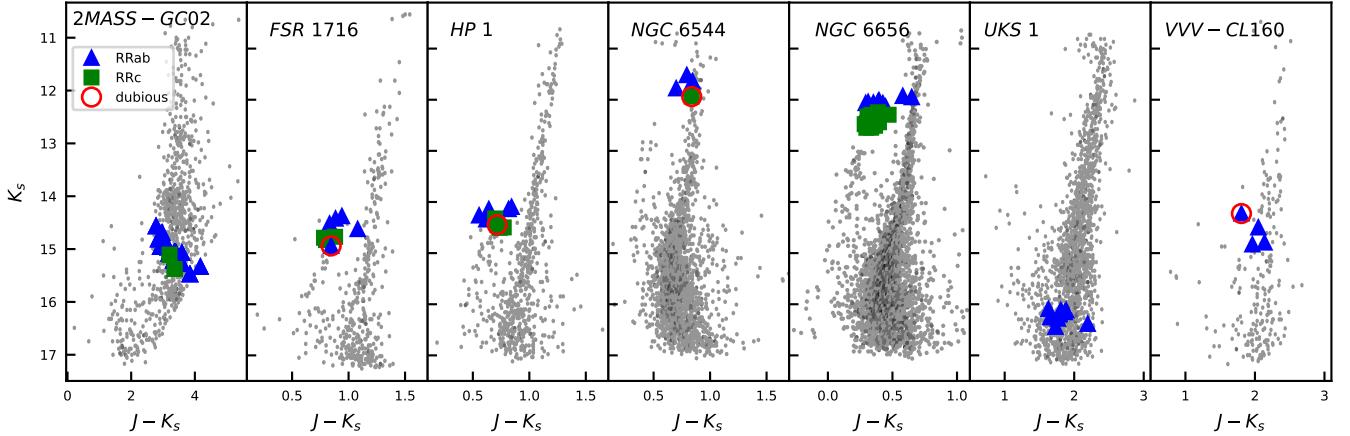
3.1. Membership assignment

We still needed to identify which of the VIVACE RR Lyrae stars detected in the vicinity of the VVV GCs are indeed members of the clusters. To do this, we modified to some extent the procedure we followed in Paper II. We began by selecting all the VIRAC2 sources located inside the tidal radius of the different clusters in our sample. However, unlike in Paper II, we now rely on the more recent coordinates and tidal radii R_t for the Galactic GCs provided in the 4th version of the Galactic Globular Clusters Database[1] (GGCD; Baumgardt & Hilker 2018) as given in Table A.1. Taking the proper motions (PM) and corresponding errors of the sources for a given cluster reported in VIRAC2, which include the VIVACE variable stars, we used extreme deconvolution Gaussian mixture modeling (XDGMM; Holoien et al. 2017) to assign a probability of cluster membership to every selected VIRAC2 source. Although in Paper II we used a k-nearest neighbor (kNN) algorithm, in the present paper we opted for the XDGMM algorithm, as the distribution of stars from the GC and the field are well represented by such mixture models in the PM space (Vasiliev & Baumgardt 2021). This algorithm also allows us to incorporate PM errors, which VIRAC2 provides. We modeled the stellar PM distribution with two Gaussian functions: the narrower one corresponds to the stars in the GC and the wider one to the stars in the field. The VVV GCs show a broad range of masses and brightnesses (see Table A.1), and the field density at the sky positions of the different GCs varies significantly (Alonso-García et al. 2018). However, defining the training sample for the GCs to contain only stars close to their centers ($r \leq 0.75' - 2'$) and with well-determined VIRAC2 PMs ($\sigma_{\mu_{\alpha*}} < 1$ mas yr^{-1}, $\sigma_{\mu_\delta} < 1$ mas yr^{-1}), we obtained good definitions for both field and cluster PM distributions in the VVV GCs.

Unfortunately, for most of the VVV GCs the PM distribution of the cluster stars shows some overlapping with that of the field stars, which does not allow for a completely clean selection (see Sect. 4.2). Therefore, we need to use additional methods to refine our membership assignment. Proximity to the cluster center also increases the probability for a star to be a cluster member (Alonso-García et al. 2011). However, keeping only RR Lyrae stars close to the cluster center would undermine our goal, which is to characterize all the RR Lyrae variables belonging to the VVV clusters. As another means to check on their GC membership, we can also use the RR Lyrae tight near-infrared PLZ relations, which once applied would result in significant groupings in their distance moduli (see Sect. 6).

To determine the GC membership of the sampled RR Lyrae stars, we define a method that makes use of all this information. First, we select only those that belong to a given VVV GC according to the PM XDGMM algorithm (probability >0.5), which are in the inner regions of the cluster, no more than two half-light radii from its center ($r < 2R_h$), and whose distance moduli, according to their PLZ relations, agree within a 3-sigma clipping mean. Once this initial approximation to the GC distance is established, we relax the requirement about the projected distance to the GC center to include all RR Lyrae stars within

---

[1] https://people.smp.uq.edu.au/HolgerBaumgardt/globular/

Fig. 1. Near-infrared CMDs for selected VVV GCs with assigned RR Lyrae members. The diagrams include only stars located in the innermost GC regions ($r \leq 1.0'$), selected as candidates by our PM XDGMM classifier. RR Lyrae stars for each GC are overplotted, with RRab stars represented as blue triangles and RRc stars as green squares. Dubious candidates are highlighted with red circles. A complete version of this figure, showing all 26 VVV GCs with assigned RR Lyrae members, is provided in Fig. B.1.

the GC ($r < R_t$) fulfilling the other two requirements. We report these RR Lyrae stars as bona fide cluster members in Sect. 5.

We also report as dubious cluster candidates those RR Lyrae stars located within the innermost regions of the GCs ($r < 2 R_h$) that fulfill at least one of the other two requirements: membership based on PM or based on the distance moduli derived from the PLZ relations. Although in principle those pulsators should not be considered as cluster members, we decided to consider them as potential candidates as the photometry or astrometry of the stars in the core of the GCs is sometimes not well defined in VIRAC2 due to the very high crowding of these regions (Majaess et al. 2012a,b).

Finally, for GCs with only one RR Lyrae star located in the inner regions ($r < 2 R_h$) and with appropriate PM, we consider these classical pulsators as possible candidate members, as we are unable to apply the membership procedure based on the PLZ relations.

3.2. Distance determination

As mentioned in the previous sections, we can find the distance to the RR Lyrae stars using their near-infrared PLZ relations. In Paper I, we defined a set of PLZ relations calibrated in the VVV filter system, which we slightly recalibrated in Paper II. To use these relations, in addition to the magnitudes and periods of the RR Lyrae stars provided by VIVACE, we also need their metallicities. We obtained them applying Eq. (1) in Navarrete et al. (2017), which required the iron content [Fe/H] and the α-enhancement [α/Fe] of the RR Lyrae stars. We assumed a common metallicity for all the stars in a given GC. For the iron content, we used the [Fe/H] values in Table A.1 derived mainly from Schiavon et al. (2024) based on APOGEE DR17, complemented by other recent spectroscopic studies (see Table A.1). As for the α-enhancement, we assumed an [α/H] = 0.3 for all GCs. The periods of the RRc stars also needed to be fundamentalized using the relation $\log P_{ab} = \log P_c + 0.127$ (Del Principe et al. 2006; Navarrete et al. 2017).

To properly calibrate our PLZ relations, we apply them to the RR Lyrae stars associated with NGC 6656 (M 22) and compare the results with the distance provided by *Gaia* measurements in the GGCD. This approach follows the method we used to recalibrate the PLZ relations in Paper II. To align the two sets of

distances for M 22, we found we need to apply a slight offset $\Delta M = -0.026$ to the PLZ relations from Paper II, transforming them into

$$M_{K_s} = -0.506 - 2.347 \log(P) + 0.1747 \log(Z), \quad (1)$$

$$M_H = -0.423 - 2.302 \log(P) + 0.1781 \log(Z), \quad (2)$$

$$M_J = -0.105 - 1.830 \log(P) + 0.1886 \log(Z), \quad (3)$$

$$M_Y = +0.140 - 1.467 \log(P) + 0.1966 \log(Z), \quad (4)$$

$$M_Z = +0.288 - 1.247 \log(P) + 0.2014 \log(Z). \quad (5)$$
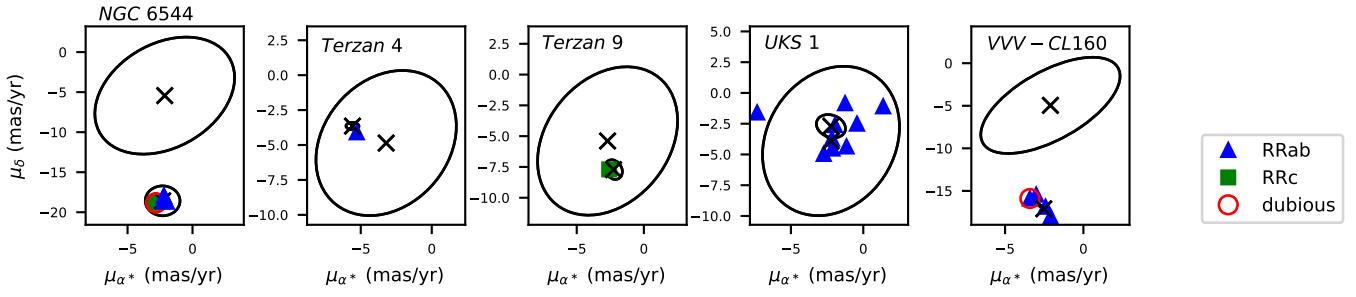
We chose M 22 as the reference because, as we detail in Sect. 6, this is the GC in our sample whose distance was obtained using the most methods from *Gaia* and *Hubble* Space Telescope (HST) measurements (Baumgardt & Vasiliev 2021) and also contains the highest number of references from the literature in the distance provided by the GGCD.

4. CMDs and PM in the VVV GCs

The 41 GCs in the 4th version of the GGCD that fall in the footprint of the VVV survey exhibit a diverse range of physical and observational parameters (see Table A.1). In this section we will present the CMDs and the PM vector-point diagrams (VPDs) of the stars in the VVV GCs, focusing on the positions of the cluster RR Lyrae stars in them.

4.1. CMDs of the VVV GCs

Since it is constructed using PSF photometry, the VIRAC2 catalog allows us to recover deeper and more complete near-infrared CMDs for the VVV GCs (Alonso-García et al. 2018). We present these CMDs in Figs. 1 and B.1 for the VVV GCs with RR Lyrae stars, and in Fig. B.2 for those with no detected RR Lyrae stars in them. Due to the low Galactic latitudes where they all lie, field star contamination is significant. To minimize this effect in our CMDs, we plot only stars in the inner regions of the GCs ($r \leq 1'$) that are considered members according to the PM analysis from our XDGMM algorithm (membership probability > 0.5). The

Fig. 2. VPDs showing the PM of the RR Lyrae cluster members of selected VVV GCs. RRab stars are represented as blue triangles, while RRc stars are shown as green squares. Red circles indicate dubious candidates. Ellipses representing the 2σ distributions of field and cluster stars, as determined by our XDGMM algorithm, are overplotted, with crosses marking the centers of both distributions. A complete version of this figure, showing all 26 VVV GCs with assigned RR Lyrae members, is provided in Fig. C.1.

short exposure times in the VVV survey makes our near infrared VIRAC2 photometry deep enough to only reach the upper main sequence above the magnitude confusion limit for two relatively nearby clusters, NGC 6544 and NGC 6656 (M 22). However, we do reach the more evolved regions of the red giant branch (RGB) and horizontal branch (HB) for all of them. Therefore, we are covering with our VIRAC2 photometry the region where the RR Lyrae stars are located in these GCs, and VIVACE should have been able to identify them. Even in the highly reddened, distant cluster UKS 1, VIVACE detects a significant number of RR Lyrae stars just over the detection limit. On the other hand, for the aforementioned nearby NGC 6544 and M 22, VIVACE finds RR Lyrae stars just below the saturation limit (see Figs. 1 and B.1). There are 15 GCs in our sample for which our analysis does not identify any member RR Lyrae stars (see Fig. B.2). Most of them are metal-rich GCs that show very red HBs in their CMDs, which do not reach the bluer colors of the RR Lyrae stars. This is the case of Liller 1, NGC 6440, NGC 6528, NGC 6553, NGC 6624, NGC 6637, Pal 6, Terzan 2, Terzan 6, Terzan 12 and Ton 2, all of them with [Fe/H] > −0.92 as shown in Table A.1. The other GCs which do not present any RR Lyrae stars show very poorly populated CMDs in their inner regions, where we expect to find most of these pulsating stars. This is the case of Djorg 1, Gran 1, Gran 5, and VVV-CL001. On the other hand, in the other 26 GCs in our sample we were able to identify RR Lyrae stars (see Fig. B.1). These metal-poor GCs (−1.70 < [Fe/H] < −0.78) present CMDs that, in general, show well-populated RGBs and blue HBs. But even in some cases where the CMDs are more scarce in members, we could identify at least one RR Lyrae candidate (e.g., BH 261, Terzan 4, or Terzan 9).

4.2. PM of the VVV GCs

In our VIRAC2 dataset, the VPDs of the PM of the VVV GCs generally show highly clumped distributions for cluster stars, superimposed on a wider distribution of field stars, as observed in Figs. 2 and C.1. Such PM distributions help to detect field stars with PM incompatible with being cluster members; however, for stars with PM compatible with being members, they do not allow for a clear discrimination between cluster and field stars, even at projected distances relatively close to the cluster centers as field stars rapidly dominate over cluster members at these low latitudes. Accurate PM separation is even more complicated for the VVV GCs where the centers of the cluster and field distributions are very close, as in NGC 6380, NGC 6441, NGC 6528, or NGC 6638. On the other hand, a few VVV GCs

has clearly separated PM distributions of cluster and field stars (e.g., 2MASS-GC02, NGC 6544, NGC 6656, VVV-CL160), which allows for a more reliable identification of the GCs' stellar populations, including their RR Lyrae variables, extending to their outer regions.

As a by-product of our cluster membership assignment, we obtained the PM of the VVV GCs. In Table C.1, we present the PM we derived by applying the XDGMM algorithm on the VIRAC2 data. We observe good agreement with the GGCD data obtained from *Gaia*, except for UKS 1 and 2MASS-GC 02. These two GCs show some of the highest extinctions among the VVV GCs, as we can infer from their very reddened CMDs (see Fig. B.1) and will detail further in Sect. 6. Therefore, observing these GCs at optical wavelengths with *Gaia* is highly challenging, and misidentification of cluster members may have led to incorrect PM assignment. On the other hand, the VIRAC2 near-infrared data from these GCs allow for a clearer identification of their members. We previously observed this same effect for 2MASS-GC 02 in Paper II and for UKS 1 in Fernández-Trincado et al. (2020).

5. RR Lyrae stars in the VVV GCs

Even though all 41 VVV GCs have RR Lyrae stars identified by VIVACE inside their tidal radii, only in 26 of them we identified any bona fide RR Lyrae members after performing the analysis detailed in Sect. 3. We summarize the number of detections of the different types of RR Lyrae stars in these 26 VVV GCs in Table D.1 and compare them to the most updated version of the Catalogue of Variable Stars in Globular Clusters (CVSGC; Clement et al. 2001) or, when available, more recent references from the literature. Table D.2 reports the main observational parameters of the VVV GC RR Lyrae stars as reported by VIVACE, along with a flag reporting on their membership assignment based on the analysis in Sect. 3. We present in Figs. 1 and B.1 the CMDs of the VVV GCs with the positions of the detected RR Lyrae stars superimposed. Additionally, we also present the VPDs of the PM of the cluster RR Lyrae stars, along with the distributions of the field and cluster populations, in Figs. 2 and C.1. In the following subsections we discuss in more detail the characteristics of the detected RR Lyrae stars in the individual VVV GCs. In particular, we emphasize the comparison of our membership assignments with those from the recent studies by Cruz Reyes et al. (2024) and Prudil & Arellano Ferro (2024), which use the third data release (DR3) from the *Gaia* mission to characterize and assign membership to RR Lyrae stars in the Galactic globular clusters.

5.1. 2MASS-GC02

We previously explored the variable stars in 2MASS-GC02 in Paper I and Paper II. VIVACE lists all the RR Lyrae stars that we found in those papers. Our analysis identifies 16 RRab and two RRc as bona fide cluster members. All the RRab considered cluster members in Paper I and Paper II are identified, plus two new RRab (1020301 and 1020311)[2] and also, for the first time, two RRc (1020312 and 1020316) in this GC. We include them in Tables D.1 and D.2 as bona fide members. There is one more VIVACE RRab, 1020332, which lies near the cluster center ($R < 1.58' = 1.1\,R_h$), with a high probability of being a cluster member according to our PM analysis. However, the distance and color inferred from the PLZ relations do not agree with those of the other RR Lyrae stars, so we include it as a dubious candidate in Tables D.1 and D.2. There are 13 RRab in the CVSGC for this GC, taken from our Paper I. We considered 12 of them as cluster members in both Paper I and Paper II, but we pointed out in both papers that V31, the RRab farthest from the cluster center in projection, should be considered a field star. Our current analysis further confirms this fact, and we flagged this star in Table D.2 accordingly. Neither Cruz Reyes et al. (2024) nor Prudil & Arellano Ferro (2024) include 2MASS-GC02 in their analysis, due to its high reddening.

5.2. BH 261 (AL 3)

BH 261 does not appear in the CVSGC, but in the recent study of this GC by Kunder et al. (2024), they found one RRc star that they considered a member. Cruz Reyes et al. (2024) also identify this pulsator in their Gaia sample as a cluster member. VIVACE lists this variable star, alongside other pulsators within the tidal radius of this GC. However, after applying our XDGMM algorithm to the PM, only 778882, the RRc found by Kunder et al. (2024) and Cruz Reyes et al. (2024), is assigned to BH 261. This is also the closest pulsator to the cluster center ($r = 0.37'$), and the only one within its half-light radius, which reinforces its probability of belonging to the cluster.

5.3. Djorg 2

The CVSGC lists five RRab and two RRc for Djorg 2, taken from the OGLE variable star database (Soszyński et al. 2014) based on their relative distance to the cluster center ($r < 2'$). VIVACE only detects three of these RRab: V1=784125, V2=784166, and V5=786666. These are the only VIVACE pulsators for this GC that our analysis considers as cluster members. Cruz Reyes et al. (2024) also identify these three pulsating stars as cluster members, but Prudil & Arellano Ferro (2024) only recognize V2 as a member in their study.

5.4. FSR 1716 (VVV-GC05)

FSR 1716 does not appear yet in the CVSGC, but its variable population has been recently explored by our collaboration. Minniti et al. (2017) found 12 RRab that they tentatively assigned to the cluster based on their projected proximity. Contreras Ramos et al. (2018), using PM analysis, refined the assignment, keeping six RRab and three RRc as cluster members. VIVACE finds all of these variable sources, but our PM analysis only considers five RRab and three RRc as members, all included in the Contreras Ramos et al. (2018) selection. These eight RR Lyrae

stars are also the closest to the GC center, with $r < 2\,R_h$, and their PLZ relations suggest a common distance (see Fig. E.1). We include them in Tables D.1 and D.2 as bona fide members. However, although they are all included in the study by Cruz Reyes et al. (2024), it is worth noting that they are classified as non-members in their analysis. Additionally, we point out that the three variable stars from Minniti et al. (2017) that both Contreras Ramos et al. (2018) and we disregard as cluster members are not even considered RR Lyrae stars but eclipsing binaries by VIVACE. There is also another RRab in Minniti et al. (2017), 1231449=d025-0114911, which our XDGMM algorithm disregards as a cluster member, while Contreras Ramos et al. (2018) do not, based on its PM. Cruz Reyes et al. (2024) do not list it in their sample. This RRab is much further from the cluster core ($r < 11.6' = 6.8\,R_h$) and its period is much shorter than that of the other RRab members, but its PLZ relations suggest a common distance modulus with the other RR Lyrae stars in the cluster. However, based on the selection criteria we listed in Sect. 3, we do not consider it a member.

5.5. FSR 1735 (2MASS-GC03)

FSR 1735 does not appear yet in the CVSGC, but in our VVV collaboration, Carballo-Bello et al. (2016) explored this GC and found three candidate RRab in its neighborhood. VIVACE identifies all these RR Lyrae stars[3], but our analysis considers as cluster members only V1=1129841 and V2=1129823, the two closest pulsators to the GC center ($r < 1.2\,R_h = 1.2'$). We include them in Tables D.1 and D.2 as bona fide members. Our analysis discards V3=1129230, which in addition to being located far from the center ($r \sim 8\,R_h = 8.2'$), has a low probability of being a cluster member according to the PM analysis. In their study, Cruz Reyes et al. (2024) classify only V1 as a cluster member.

5.6. HP 1 (FSR 1781)

Our analysis identifies six RRab and three RRc as bona fide cluster members of HP 1, which are listed in Tables D.1 and D.2. Additionally, we classify one RRc, 290373, as a dubious member. Although it lies near the cluster center ($r \sim 1.2' = 0.8\,R_h$) and its distance modulus, based on the PLZ relations, is consistent with that of the other RR Lyrae members (see Fig. E.1), the XDGMM analysis of the PM assigns it a low membership probability. We have flagged this star accordingly in Table D.2. The CVSGC does not list any RR Lyrae stars for HP 1. However, Kerber et al. (2019) provided a comprehensive study of this GC, including its variable population. Taking the RR Lyrae stars that are closer than 150″ from the cluster center in the OGLE catalog (Soszyński et al. 2014), they found six RRab and five RRc compatible with being cluster members. VIVACE detects all but two RRc stars from their selection. Our analysis, however, does not classify two RRab, OGLE-BLG-RRLYR-19433=290346 and OGLE-BLG-RRLYR-19503=290374, as members, and we have flagged them as non-members in Table D.2. Vásquez Zapata (2021), in her M.Sc. thesis, also studied the variable population of HP1 using VVV observations. She reported 18 variable stars as potential cluster members, including eight RRab and four RRc stars. VIVACE misses one RRab (HP1-9) and one RRc (HP1-10) from her list. And while our analysis considers one of her listed RRab, HP1-17=290229, as a field star, we confirm two RRab (HP1-14=290365 and HP1-5=290369) as bona fide

---

members previously unreported by Kerber et al. (2019). Lastly, Cruz Reyes et al. (2024) also listed six RRab and five RRc as HP 1 members. VIVACE misses one RRc, the same as in the two previously cited studies, but our analysis confirms the cluster membership of another RRc (290366), which had not been reported by either Kerber et al. (2019) or Vásquez Zapata (2021).

5.7. NGC 6380 (Ton 1)

Our analysis assigns seven RRab and three RRc as bona fide members of NGC 6380, and one additional RRab as a dubious member. We list them in Tables D.1 and D.2. There are no RR Lyrae stars associated with NGC 6380 according to the CVSGC, but using OGLE data, Soszyński et al. (2019) consider as members the nine RR Lyrae stars inside their considered cluster radius ($r < 3.6'$). The region we explore, extending out to the tidal radius ($R_t = 14.4'$, see Table A.1) is significantly larger. We emphasize that we classify as bona fide cluster members all the inner RR Lyrae stars from the OGLE catalog cited by Soszyński et al. (2019) for this GC, except for OGLE-BLG-RRLYR-51429, which is the closest to the cluster center and that VIVACE fails to identify. Cruz Reyes et al. (2024) also classifies as cluster members the three RRab and three RRc in common. Adding to those, there are three RRab (85269, 85270, and 90714) in the outskirts of NGC 6380 ($4.1' \leq r \leq 12.4'$) that we classify as cluster members. The RRab 85269 is also classified by Cruz Reyes et al. (2024) as a cluster member, but the other two are newly discovered cluster candidates. The farthest of these from the cluster center, 90714, has a borderline probability (46%) of belonging to the GC according to the PM analysis, so we flag it as a dubious candidate.

5.8. NGC 6401

NGC 6401 is rich in RR Lyrae stars. Our analysis considers 21 RRab and three RRc in VIVACE as bona fide members of NGC 6401, plus two more RRab and one RRc as dubious members. They are all included in Tables D.1 and D.2. The CVSGC for NGC 6401 reports 23 RRab and 11 RRc, taken from the recent variability study by Tsapras et al. (2017). VIVACE fails to detect four RRab and seven RRc, most of which are located in the very core of the cluster. Among the 19 RRab and four RRc that VIVACE detects in common with the CVSGC, all of them are considered cluster members by our analysis, except for one RRab, V17=564279, which has been flagged in Table D.2 as a field star. However, there are two RRab in this group (V32=563533 and V34=564266) whose position in the very core of the cluster and PM probabilities suggest they are cluster members, but whose distance moduli are ~0.2 mag smaller than the others. However, their mean K_s magnitude reported in VIVACE may have easily been affected by the high crowding of the core. Likewise, there is also another RRc, V23=564278, whose position near the cluster core ($r = 2.2' \sim 2.1 R_h$) and distance modulus according to the PLZ relations put it inside the cluster (see Fig. E.1), but whose PM do not agree with those of NGC 6401, raising a question about its membership. We report these three RRab as dubious cluster member candidates in Tables D.1 and D.2. Additionally, we include five more RRab (563525, 564296, 558881, 558882, and 564302) as bona fide cluster members which do not appear in the CVSGC. The reason for their omission may have been their location outside the radius $R = 2.4'$ where Tsapras et al. (2017) focused their search for cluster members. These five pulsating stars, however, were identified and classified as cluster members in

Aravena Rojas (2020), who used VVV data in his M.Sc. thesis to study NGC 6401, and later in Cruz Reyes et al. (2024). We note the case of the RRab 564302. The period reported by VIVACE appears to be aliased, as it is close to twice the value reported by OGLE, *Gaia*, and Aravena Rojas (2020). We consider it a bona fide cluster member, as its PM analysis shows a high probability of membership and the PLZ relations, when including the recalculated period, places this star at a distance consistent with the other RR Lyrae members. Finally, we note that Aravena Rojas (2020) agrees with our membership assignments for all common RR Lyrae stars. However, for Cruz Reyes et al. (2024) and Prudil & Arellano Ferro (2024) there are a few stars for which our membership assignments differ. Differently from our analysis, Cruz Reyes et al. (2024) classify V17 as a cluster member and V16, V22, V29, and V32 as field stars, while Prudil & Arellano Ferro (2024) consider V2, V6, V23, V26, V32, and V34 as field stars.

5.9. NGC 6441

Along with NGC 6388, NGC 6441 forms the Oosterhoff III group of high-metallicity GCs that contain a significant number of long-period RR Lyrae stars (Pritzl et al. 2000). Our analysis identifies 20 RRab and five RRc as bona fide members of NGC 6441 among the VIVACE variables, plus two additional RRab and one RRc as dubious members. These stars are all included in Tables D.1 and D.2.

The CVSGC for NGC 6441 lists 44 RRab (plus three more possible RRab), 19 RRc (plus seven more possible RRc), one RRd, and two RR Lyrae with no subtype classification. This high number of RR Lyrae stars was discovered mainly in the innermost GC by Pritzl et al. (2003), who took full advantage of the superb resolution of the HST. Our ground data misses most of the stars located in the innermost GC regions, detecting only two pulsators of the 55 listed at $r < 1.0'$. However, VIVACE detects most of the cluster members at $r > 1.0'$, missing only two RRab (V41 and V97) and three RRc (V71, V74, and V102). We note that the coordinates of two RRab members (V40 and V59) differ by more than $1''$ between CVSGC and VIVACE. Moreover, there are five additional stars classified as RR Lyrae members in the CVSGC but that VIVACE classifies as eclipsing binary stars (V52, V78, V93, V96, and V150). After examining their light curves, we considered these as misclassifications from VIVACE and recalculate the period following Paper II. We treat them as bona fide RR Lyrae members, as their PM and distances derived from the PLZ relations are consistent with those of other RR Lyrae members. Similarly, V69 is classified as an RRab by VIVACE and as an RRc in the CVSGC. Although its period seems to match an RRab, its low amplitude suggests it is an RRc. We retained this classification, as it places the star at the GC distance based on the PLZ relations. We had a similar discussion about this star in Paper II. All these variable stars, for which we modified their variability classification, are flagged in Table D.2.

The CVSGC also lists three RRab (V36, V54, and V67) and two RRc (V68 and V73) as possible field members in NGC 6441. VIVACE detects them as well, and our analysis confirms that they are not cluster members. We have flagged these stars in Table D.2. There are three more RR Lyrae stars from the CVSGC whose distance moduli from the PLZ relations set them as field stars, although they could be members according to PM and distance to the center: V45, V49, and V70. As we noted earlier, PM separation between cluster and field stars for NGC 6441 is complicated, so we prefer to consider them as field variable stars, as we did in Paper II. On the other hand, one RRab (V53) and one

RRc (V77) are located in the inner regions of the cluster, and their distance moduli based on the PLZ relations place them as cluster members, but their XDGMM probabilities are low. We include them as dubious members in Tables D.1 and D.2.

We previously studied NGC 6441 in Paper II and reaffirm our membership assignments for all the stars in common, including an additional RRab, C36=105687, which was first reported as a member in Paper II. We also agree with the membership assignment of Oliveira et al. (2022) for all the RR Lyrae stars in common, except for V45, V66, V70, and V72. They also report a newly classified RRc member, OGLE-BLG-RRLYR-30179, which is not detected by VIVACE. Cruz Reyes et al. (2024) list one additional new RRab member, Gaia-4040152937984200576, but although VIVACE detects it (105236), our analysis considers it a field star. For the stars in common, all our bona fide members are also considered cluster members by Cruz Reyes et al. (2024), except V40, V42, and V66. On the other hand, all of our field RR Lyrae stars are considered cluster members by Cruz Reyes et al. (2024), except V70. For our two dubious members in common, Cruz Reyes et al. (2024) classify V77 as a member, but considers V53 a field star. We also compared our membership assignments with those of Prudil & Arellano Ferro (2024) and found disagreements for a significant number of RR Lyrae stars: V37, V39, V43, V51, V53, V62, V66, V70, V72, V77, and V93.

Finally, we highlight that we consider three RRab (105175, 105856, and 198097) and one RRc (105528) as newly classified members of NGC 6441. While all of them are considered members according to their PM by our XDGMM classifier and the PLZ relations set them at the right distance, we notice that they are quite far from the cluster core ($16.6' \leq r \leq 25.9'$), which is probably the reason for having been missed before. Since one of these RRab, 198097, has a borderline probability (44%) of belonging to the GC according to the PM analysis, we flagged it as a dubious candidate.

5.10. NGC 6453

The CVSGC lists three RRab and five RRc for NGC 6453. As with other GCs, VIVACE misses most of the variables in the inner regions ($r < 1'$), but detects the majority of the pulsators that are beyond. Unfortunately, this leaves us with only one RRab, V8=207475, which our analysis classifies as a bona fide cluster member. There are other two pulsators, the RRab V4=207471 and the RRc V3=207472, near the center of the cluster ($r < 1.5' = 1.6\,R_h$) and located at the same distance as V8 according to the PLZ relations (see Fig. E.1), but having low probabilities of belonging to the cluster according to their PM. Thus, we classify them as dubious cluster members in Tables D.1 and D.2. Both Prudil & Arellano Ferro (2024) and Cruz Reyes et al. (2024) classify V4 and V8 as cluster members, but consider V3 a field star. VIVACE also detects two additional CVSGC RRc, V5=207460 and V6=207459, but our analysis considers them field stars. Prudil & Arellano Ferro (2024) agree with this classification, while Cruz Reyes et al. (2024) classify them as cluster members.

5.11. NGC 6522

Our analysis classifies four VIVACE RRab and three VIVACE RRc as bona fide members of NGC 6522. We list them in Tables D.1 and D.2.

According to the CVSGC for this cluster, it harbors five RRab and six RRc. VIVACE fails to identify two RRab (V10 and V11) and two RRc (V12 and V14), likely due to their very central location ($r < 0.3'$ for V10, V11 and V14). The rest of the CVSGC RR Lyrae stars for NGC 6522 appear in VIVACE and we classify all but one RRc, V9=735496, as cluster members (see Table D.2). Furthermore, we identify one RRab member, V4=736543, with an offset of $2''$ from the position provided in the CVSGC, as also reported by Arellano Ferro et al. (2023) in their appendix. There are six additional RR Lyrae stars reported in the CVSGC notes for NGC 6522 as found in the OGLE catalog in the vicinity of the cluster with magnitudes appropriate for cluster membership. VIVACE identifies four of them, but according to our PM analysis they have low probabilities of being cluster members.

Recently, Arellano Ferro et al. (2023) revisited the variable population of NGC 6522. For the stars in common, our membership assignments agree with theirs, including the OGLE stars listed in the CVSGC notes. They also report one additional RRc, V24, as a new member, but unfortunately, VIVACE fails to detect it. Cruz Reyes et al. (2024) also report one new RRab member, Gaia-4050201237330707712. VIVACE detects this star (737755), but our analysis classifies it as a field star, in agreement with Arellano Ferro et al. (2023). For the remaining stars in common with Cruz Reyes et al. (2024), our membership assignments agree with theirs, except for V4 and V9. In the case of Prudil & Arellano Ferro (2024), our membership assignment only differs for V2. Finally, we highlight the discovery of a new RRab member, 735495, in our data.

5.12. NGC 6540

There are two RRab and one RRc listed as members in the 2016 update of the CVSGC for NGC 6540, first discovered and assigned to the cluster by the OGLE collaboration (Soszyński et al. 2011). VIVACE detects one of the RRab, V3=796385, and the RRc, V1=796378, and our analysis considers them as cluster members. However, we note that both Cruz Reyes et al. (2024) and Prudil & Arellano Ferro (2024) consider these two pulsators as field stars. VIVACE finds another RRab, 796362, close to the cluster core ($r \sim 1.5' = R_h$), which we highlight as a new bona fide cluster member. We include it along with the other two CVSGC RR Lyrae stars in Tables D.1 and D.2.

5.13. NGC 6544

Our analysis identifies three RRab in NGC 6544 as bona fide cluster members and one RRc as a dubious member, all of which are listed in Tables D.1 and D.2. The relative proximity of this GC, inferred from its CMD (see Fig. B.1), along with its clear separation from the field in its VPD (see Figs. 2 and C.1), makes it particularly straightforward to identify the members of NGC 6544 among the VIVACE RR Lyrae stars. Only one RRab is listed for this GC in the CVSGC, which we also identify and classify as a cluster member, in agreement with Cruz Reyes et al. (2024) and Prudil & Arellano Ferro (2024). Cruz Reyes et al. (2024) also identify one additional RRab member in NGC 6544, Gaia-4065746094009651328. VIVACE detects this star (908712), and we also classify it as a bona fide member. Finally, we highlight the new identification of one additional RRab, 881126, and one RRc, 919762, as members of NGC 6544. The distance modulus to this RRc, based on the PLZ relations, is ~0.25 mag smaller than that of the other cluster RR Lyrae stars (see Fig. E.1), leading us to consider it a dubious candidate. Cruz Reyes et al. (2024) also identify this star but classify it as a field star.

5.14. NGC 6558

The CVSGC lists seven RRab and three RRc as members for NGC 6558. Since three of these stars, V9, V13 and V14, are located beyond the tidal radius for this GC (see Table A.1), we extended our search radius for RR Lyrae stars to $r = 1.6\,R_t = 6.1'$ to include them. VIVACE detects all of these stars, except V1, which is the closest to the cluster center ($r \sim 0.4'$). Our analysis classifies all these RR Lyrae stars as cluster members, except for V13=730703 and V14=731330, the two stars farthest from the GC center. We flag them in Table D.2, along with V5=730699, an RRab listed by the CVSGC as a possible field star, which we also detect and classify as a non-member variable star. All the other RR Lyrae stars (six RRab and one RRc) are considered bona fide members of NGC 6558, and listed in Tables D.1 and D.2. Notably, this includes V9=730641, which lies outside the tidal radius of the cluster ($r = 5.9' = 1.5\,R_t$).

When comparing our membership assignments with recent studies, we find a general agreement for most stars in common, with a few exceptions: V8 and V9 with Arellano Ferro et al. (2024); V4 with Prudil & Arellano Ferro (2024); and V5, V13, and V14 with Cruz Reyes et al. (2024). Finally, there is an additional RRab detected by VIVACE, 730683, with no counterpart in the CVSGC. Although it has low probability of being a cluster member according to our PM analysis, it lies relatively close to the GC center ($r \sim 1.1' = 1.2\,R_h$) and its distance modulus, based on the PLZ relations, agrees with those of the other RR Lyrae members (see Fig. E.1). We include it in Tables D.1 and D.2 as a dubious member. However, we note that only Arellano Ferro et al. (2024) list it (O47), but classify it as a field star.

5.15. NGC 6569

Our analysis identifies seven RRab and three RRc in NGC 6569 as bona fide cluster members. We report them in Tables D.1 and D.2.

The CVSGC for NGC 6569 associates nine RRab, 12 RRc, and three possible additional RR Lyrae stars with this GC. VIVACE detects four of the RRab, three of the RRc, and one of the possible RR Lyrae, V5=731452, which it classifies as an RRab. Our analysis considers all of these as cluster members. Most of the remaining missed pulsators from the CVSGC are located very close to the central region of the cluster. VIVACE also detects two RR Lyrae stars, V6 and V19, which the CVSGC classifies as field stars. Our analysis also categorizes these as non-members, and we flag them accordingly in Table D.2. Notably, these are the RR Lyrae stars farthest from the cluster center.

In Paper II, we previously studied the variable population of this cluster. VIVACE detects all but one RRab and one RRc reported in that paper. It also detects two additional RRab, 731451 and 731496, which our analysis classifies as cluster members, previously reported as such in Paper II (variables C2 and C13, respectively), but which are still unreported in the CVSGC. Paper II agrees with our membership assignments for all common stars, while Cruz Reyes et al. (2024) disagrees for V5, V6, V19, and V20. Prudil & Arellano Ferro (2024) also agree for all stars in common, except for V5, V20 and V26.

5.16. NGC 6626 (M 28)

We identify eight RRab and six RRc as bona fide members of NGC 6626, along with two additional RRab and one

RRc as dubious members. We include them all in Tables D.1 and D.2.

According to the CVSGC, this GC hosts ten RRab and eight RRc. VIVACE misses only four RRc, all of which were newly identified by Prieto et al. (2012). Both the OGLE and *Gaia* variable star catalogs also fail to identify three of these as variables. Our analysis confirms the membership of the remaining RR Lyrae stars in the CVSGC, with the exception of three RRab (V9=969821, V18=969858, and V20=969859), which have low probabilities of being cluster members according to their PM. However, we classify V18 and V20 as dubious members, given their proximity to the cluster center ($r < 0.9' \sim 0.9\,R_h$) and their distance moduli, which, according to the PLZ relations, align with those of the other RR Lyrae members. Additionally, we note that two of these RRab, V20=969859 and V25=969846, show an offset of more than $1''$ compared to the positions reported in the CVSGC. VIVACE detects three additional RRab stars (V15, V16, and V24), which are classified as field stars by the CVSGC. Our analysis also categorizes them as non-cluster stars, and we flag them accordingly in Table D.2. Notably, these field RRab are located farther from the GC in projection than the confirmed RR Lyrae members.

We previously analyzed the variable population of NGC 6626 in Paper II, and identified one more RRab (969862) and three additional RRc (969825, 969826, and 969852) as cluster members. VIVACE also detects these stars, and our analysis confirms their membership in the cluster. Although one RRc, 969826, has low probability of belonging to the GC according to the PM analysis, its position near the cluster center ($r \sim 2\,R_h = 2.1'$) and similar distance modulus to the other cluster pulsators, according to the PLZ relations (see Fig. E.1), led us to consider it a probable cluster member. We include it as such in Tables D.1 and D.2. These four RR Lyrae stars are also identified as cluster variables in recent studies by Oliveira et al. (2022) and Cruz Reyes et al. (2024). For the other pulsating stars in common with our analysis, Oliveira et al. (2022) agree with our membership assignment, except for one RRc, V9. In contrast, Cruz Reyes et al. (2024) show more disagreements, including V5, V9, V15, V16, V20, V24, and V25. We also compare our membership assignments with those of Prudil & Arellano Ferro (2024), and find differences only for three stars: V5, V22, and V25.

5.17. NGC 6638

Our analysis identifies ten RRab and seven RRc as bona fide members of NGC 6638. We list them in Tables D.1 and D.2.

The CVSGC reports ten RRab and 16 RRc, along with two additional RRc classified as probable field stars for this cluster. VIVACE detects six RRab and eight RRc from this list. We note that V32=1042563 is classified as an eclipsing binary by VIVACE but as an RRab by the CVSGC. After reviewing its light curve, position in the CMD, and distance modulus derived from the PLZ relations, we could not definitively classify its variable type. Its position, very close to the cluster center ($r = 0.11'$), may introduce offsets in its photometry. Therefore, we have flagged it as a dubious variable member in Table D.2, but excluded it from Table D.1. For the remaining RR Lyrae stars in common, our analysis considers all as cluster members, except for one RRc, V38=1042556, which is classified as a field star. The two suspected field RRc identified by the CVSGC, V40=1042543 and V43=1042547, which are also detected by VIVACE, are classified as bona fide members in our analysis. Furthermore,

VIVACE classifies as RRab six variables of unknown classification in the CVSGC. Among them, the three RRab closest to the GC center, with $r < 0.5'$ (V34=1042564, V35=1042562, and V36=1042561), are classified as cluster members in our analysis, while the other three RRab (V8=1042523, V51=1042524, and V52=1042527), which are significantly farther away ($r > 7.8'$), are classified as field stars. They are flagged accordingly in Table D.2.

The variable population of NGC 6638 has been recently revisited by Oliveira et al. (2022), who identified two new RRab members in the OGLE dataset, OGLE BLG-RRLYR-62076 and OGLE BLG-RRLYR-62131, and by Cruz Reyes et al. (2024), who added one additional RR Lyrae member, Gaia-4076175962610552448. VIVACE detects one of the new RRab members from Oliveira et al. (2022), 1042546=OGLE BLG-RRLYR-62131, which our analysis also classifies as a bona fide cluster member. In comparing all RR Lyrae stars in common, our membership assignments align with those of Oliveira et al. (2022) in all cases, but disagree with Cruz Reyes et al. (2024) for V27, V30, and V38. Additionally, we find only two discrepancies with the assignments of Prudil & Arellano Ferro (2024) for V35 and V41.

Finally, we highlight our analysis includes one RRab, 1042542, as a newly identified member of NGC 6638.

5.18. NGC 6642

Our analysis identifies eight RRab and eight RRc as bona fide members of NGC 6642, along with two additional RRab and two RRc as dubious members. We list them in Tables D.1 and D.2. In the literature we note several variable stars have been detected beyond the tidal radius reported in Table A.1, which prompted us to extend the studied region out to $r \sim 1.1\,R_t = 7.6'$ to include these pulsators (see Table D.2).

According to the CVSGC, NGC 6642 contains seven RRab (plus three suspected), three RRc (plus three suspected), and one probable RR Lyrae of unclassified subtype, belonging to this GC. VIVACE detects all of the RR Lyrae stars cataloged in the CVSGC. All suspected RRab and RRc in the CVSGC are confirmed by VIVACE, and the RR Lyrae star with a previously unknown subtype is reclassified as an RRab. We observe an offset of more than $1''$ in the coordinates of V6=1046390 and V14=1046403. Additionally, we note that V4=1046405 is classified as an RRab by VIVACE but as an RRc by the CVSGC, as well as by the OGLE and *Gaia* catalogs. The period reported by VIVACE appears to be aliased, as it is three times the value provided by the other catalogs. After examining its light curve, position in the CMD, and distance modulus derived from the PLZ relations, we consider it as a misclassification by VIVACE and we classify this star as an RRc member, recalculating its period as described in Paper II, (see Table D.2). Our analysis categorizes all of the RR Lyrae star in the CVSGC for NGC 6642 as bona fide members, except for V8, V11, V17, and V18, which are classified as field stars, and V9, an RRab which is considered a dubious member due to its low membership probability based on its PM.

Using OGLE detections, Oliveira et al. (2022) recently studied this cluster and identified two new RRc members[4], OGLE-BLG-RRLYR-36604 and OGLE-BLG-RRLYR-62216. Cruz Reyes et al. (2024) classified one additional new RRab

member, Gaia-4077768914409054464. VIVACE detects all three pulsating stars (1046355, 1046368, and 1046386). Our analysis considers the two newly detected RRc as bona fide members, while the new RRab is classified as a dubious candidate, as its distance modulus, derived from the PLZ relations, shows a discrepancy with those of the other RR Lyrae members. When comparing all RR Lyrae stars in common, our membership assignments generally agree with both studies. Discrepancies occur only for V14 and OGLE-BLG-RRLYR-62390=1046394 with Oliveira et al. (2022), and for V8, V11, V17 and V18 with Cruz Reyes et al. (2024). We also align with most membership assignments by Prudil & Arellano Ferro (2024), except for V9 and V12.

Finally, we highlight the discovery of one bona fide new RRab member (1046387), one bona fide new RRc member (1046394), and two dubious RRc members (1046382 and 1046383) in NGC 6642.

5.19. NGC 6656 (M 22)

As with NGC 6544, the relative proximity of NGC 6656, evidenced by its bright sequences in the CMD (see Fig. B.1) and the clear separation between cluster and field stars in its VPD (see Fig. C.1), makes the identification of cluster members particularly straightforward. Our analysis identifies ten RRab and 13 RRc as bona fide members of NGC 6656, which are listed in Tables D.1 and D.2.

The CVSGC reports 11 RRab and 15 RRc as members of NGC 6656. All RRab are detected by VIVACE, but five RRc are missed. Additionally, there are some discrepancies in the classification of variable types. V21 is classified as an RRc by VIVACE and OGLE, but as an RRab in the CVSGC. We maintain its classification as an RRc based on its short period, small amplitude, and distance modulus from the PLZ relations (see Fig. E.1). V37 is classified as an RRab by VIVACE, but upon analyzing its light curve, we consider it an eclipsing binary, as suggested by the CVSGC and OGLE. Ku-1 is classified as an eclipsing binary by VIVACE, but after reviewing its light curve and recalculating its period following Paper II, we align it with the RRc classification provided by both the CVSGC and OGLE. Upon submitting the VIVACE-CVSGC cross-matched RR Lyrae stars to our membership analysis, we find that all of them are bona fide cluster members. It is also worth noting that NGC 6656 was studied in Paper II, where we identified the same member RR Lyrae stars, plus an additional RRc, Ku-4, which VIVACE fails to detect. The CVSGC for this GC also lists five RRab, one RRc and one RR Lyrae star with an unclassified subtype as field stars. VIVACE detects all of these stars and classifies V29=1047961, the RR Lyrae star with an unknown subtype, as an RRc, in agreement with OGLE and Paper II. Our analysis also considers all the RRab as field stars, but classifies the two RRc, V27 and V29, as bona fide cluster members, consistent with our Paper II classification.

Cruz Reyes et al. (2024) do not assign any new RR Lyrae variables as members. Our membership assignments differ from theirs only for two RR Lyrae stars, V3 and V22. On the other hand, Prudil & Arellano Ferro (2024) agree with all our membership assignments.

5.20. Terzan 1 (HP 2)

Our analysis identifies seven RRab and two RRc as bona fide members of Terzan 1, along with two additional RRab classified as dubious members. These stars are listed in Tables D.1 and D.2.

---

[4] There is one additional high-probability RRab member in Oliveira et al. (2022) with no CVSGC counterpart, OGLE-BLG-RRLYR-62397, but we believe it to be V6 based on its coordinates and reported period.

All bona fide members are located close to the cluster center ($r < 1.8' \sim 2\,R_h$).

The CVSGC for Terzan 1 includes nine RRab and three RRc. VIVACE fails to detect three RRab and all RRc, likely due to their very central location ($r < 1'$). Of the six RRab detected RRab in common, our analysis classifies V9, V15 and V17 as bona fide members, V14 as a non-member, and V7 and V10 as dubious members. Although the PM analysis indicates a high probability of cluster membership for V7 and V10, their distance moduli are ~0.2 mag smaller than those of the other RR Lyrae stars. This slight offset in their photometry may result from their close proximity to the cluster center ($r < 0.5'$).

Prudil & Arellano Ferro (2024) agree with our membership assignments for all stars, and consider our dubious members as bona fide members. In contrast, Cruz Reyes et al. (2024) disagree with our classification for V15 and V17, and classify our dubious members as field stars instead. Additionally, Cruz Reyes et al. (2024) include one extra RRab member, Gaia-4055453741758171904, which is also identified by VIVACE (326735) and is considered a bona fide member in our analysis.

Finally, we highlight the identification of three new RRab and two new RRc as bona fide cluster members. However, we note that Cruz Reyes et al. (2024) also identify one of the RRab, 326736, but classify it as a field star.

5.21. Terzan 4 (HP 4)

The CVSGC does not list any variables for Terzan 4, and Cruz Reyes et al. (2024) do not include any RR Lyrae stars for this GC either. However, one RRab listed in VIVACE, 276896, is located relatively close to the cluster center ($r \sim 2.5' = 1.7\,R_h$) and shows a high probability of belonging to the cluster according to our PM analysis. We include it as a new cluster variable candidate in Tables D.1 and D.2.

5.22. Terzan 5 (Terzan 11)

The CVSGC lists four RRab for Terzan 5, and Cruz Reyes et al. (2024) add one extra RRab, Gaia-4067312558805370624. VIVACE detects only one of these, V11=600303. Since our PM analysis assigns a high probability of cluster membership to this star, and it lies in the inner regions of the GC ($r = 1.2' \sim 1.3\,R_h$), we classify it a probable cluster member and include it in Tables D.1 and D.2. Prudil & Arellano Ferro (2024) also classify it a cluster member. The only other inner-cluster RRab in our analysis with high membership probability from its PM, and with a similar distance modulus according to the PLZ relations (see Fig. E.1), is 600304, an RRc located at $r = 2.0' \sim 2.2\,R_h$. We classify it as a new probable cluster member but note Cruz Reyes et al. (2024) consider it a field star.

5.23. Terzan 9

The CVSGC lists no variables for Terzan 9, and Cruz Reyes et al. (2024) do not include any RR Lyrae stars for this GC either. However, our XDGMM algorithm assigns a high probability of cluster membership to the VIVACE variable 805472, the RRc that is closest to the cluster center ($r = 0.3'$). We report it as a probable candidate in Tables D.1 and D.2.

5.24. Terzan 10

The CVSGC lists ten RRab and one RRc as members of Terzan 10, based on our Paper I and OGLE data

(Soszyński et al. 2014). We reexamined the variable population of this GC in Paper II, confirming the RR Lyrae members identified in Paper I. VIVACE recovers all the RR Lyrae members detected in both Paper I and Paper II (seven RRab), plus one additional RRab, V51=860441, which is included in the CVSGC from OGLE. All these stars are classified as cluster members in our analysis and are listed in Tables D.1 and D.2, along with 860314, an RRc not previously listed in the CVSGC, which our analysis also classifies as a bona fide cluster member. VIVACE also detects V12, an RRab that is classified as a field star in the CVSGC. Our current analysis similarly classifies it as a field star, and we flag it as such in Table D.2. Prudil & Arellano Ferro (2024) agree with most of our membership assignments but classify V12 and V51 differently, and they are unable to classify V6 and V24. In contrast, Cruz Reyes et al. (2024) classify all variables stars listed in the CVSGC for Terzan 10 as field stars.

5.25. UKS 1 (FSR 16)

We highlight the discovery of a significant RR Lyrae variable population in UKS 1. Neither the CVSGC nor Cruz Reyes et al. (2024) list any variable stars for this GC. However, our analysis of the VIVACE RR Lyrae stars identifies nine RRab as bona fide cluster members, which we have included in Tables D.1 and D.2. While most of these stars are concentrated near the cluster center ($r < 1.9' \sim 2.9\,R_h$), a few are located in the outskirts of the cluster. Notably, their magnitudes are near the confusion limit, which could account for the absence of a distinct HB in our CMD for this GC (see Fig. B.1).

The average period of its RRab stars, 0.57 days (see Table D.2), and its reported iron content, [Fe/H] = −1.0 dex (see Table A.1), classify UKS 1 as a new member of the Oosterhoff I group (Catelan & Smith 2015).

5.26. VVV-CL160

We highlight the discovery of RR Lyrae stars for VVV-CL160 in our analysis. This GC has not yet been included in the CVSGC, as it was only recently confirmed as a new Milky Way GC by Minniti et al. (2021). Although Garro et al. (2022) examined it for RR Lyrae stars using the OGLE database, no variables were found. Similarly, Cruz Reyes et al. (2024) do not list any RR Lyrae stars for this GC. However, VIVACE lists several newly detected RR Lyrae stars within the tidal radius of VVV-CL160, and our PM analysis identifies the four RRab closest to the GC center ($r < 2.0' = 1.3\,R_h$) as highly probable members. The PM separation between cluster and field stars for VVV-CL160 is particularly distinct (see Sect. 4.2), indicating a highly significant membership distinction. Three of these RRab also have similar distance moduli (see Fig. E.1), and we classify as bona fide cluster members in Tables D.1 and D.2. The fourth RRab, 1055884, has a distance modulus derived from the PLZ relations that is significantly smaller ($\Delta(K_s - M_{K_s}) \sim 0.5$ mag), suggesting a shorter distance than the others, so we flagged it as a dubious member.
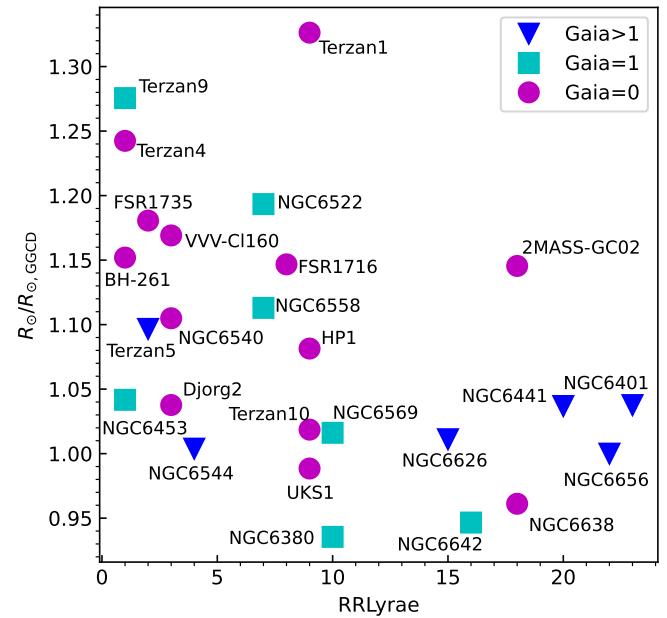
6. Distances and extinctions to the VVV GCs

We have used the near-infrared PLZ relations from Sect. 3.2 along with the VIVACE periods and apparent magnitudes of the RR Lyrae stars in the VVV GCs in Table D.2 to infer their apparent distance moduli and color excesses (see Fig. E.1). To obtain the true distance to these RR Lyrae stars, and therefore the distance to their parent GCs, we need to correct for their

color excesses using an extinction law. Extinction at low latitudes toward the Galactic center varies non-canonically (Nishiyama et al. 2006; Alonso-García et al. 2017; Nogueras-Lara et al. 2018; Dékány et al. 2019). Recently, Sanders et al. (2022) recalibrated the infrared extinction law values in a sizable region of 3×3 deg^2 around the Galactic center using VVV, GLIMPSE and WISE data. In our analysis we assume a Cardelli et al. (1989) canonical extinction law for the VVV GCs located farther from the Galactic plane ($|l| > 5°$) and a Sanders et al. (2022) non-canonical extinction law for those located at lower latitudes ($|l| > 4°$), except for 2MASS-GC02, whose very severe differential extinctions (see Fig. B.1) enable us to measure the selective-to-total extinction ratios directly. As we did in Paper I and Paper II, we perform an ordinary least-squares bisector fit to the distance moduli and color excesses of the RR Lyrae stars in 2MASS-GC02 inferred from the PLZ relations (see Fig. E.1). This results in selective-to-total extinction ratios of $R_{K_s,H-K_s} = 1.20 \pm 0.11$ and $R_{K_s,J-K_s} = 0.56 \pm 0.06$ as the slopes of the linear fit. These values are in agreement with those we derived in Paper I and Paper II.

The weighted average distances and color excesses of all the RR Lyrae stars in a given GC are provided in Table E.1, along with their galactocentric distances, which we obtained assuming an $R_0 = 8275 \pm 9 \pm 33$ pc (GRAVITY Collaboration 2021). For GCs with more than one RR Lyrae star, only bona fide members were used to obtain their parameters, excluding the RR Lyrae stars flagged as dubious candidates. As expected, the GCs located closer to the Galactic plane exhibit higher reddenings. Even though at near-infrared wavelengths extinction is diminished, color excesses increase from $E(J - K_s) < 0.2$ mag for GCs at $|l| > 5°$ up to values of $E(J - K_s) \sim 1.0$ mag for GCs closer to the Galactic plane, reaching mean values as high as $E(J - K_s) = 1.57$ mag for UKS 1, $E(J - K_s) = 1.79$ mag for VVV-CL 160, and even $E(J - K_s) = 3.04$ mag for 2MASS-GC02, our most reddened GC. Distances to the GCs place the vast majority of them within the Galactic bulge, at distances from the Galactic center $R_{GC} < 3$ kpc (see Table E.1). The only GCs in our sample outside the Galactic bulge realm are the nearby NGC 6544 and NGC 6656, the highly reddened 2MASS-GC02, as well as the distant UKS 1 and NGC 6441. Conversely, there are five GCs (FSR 1716, NGC 6380, NGC 6401, NGC 6558, and NGC 6642) located in the innermost regions of the bulge, at distances $R_{GC} < 1$ kpc.

We compared the distances to the VVV GCs that we obtained from the RR Lyrae stars with those reported in the GGCD, which were taken mainly from Baumgardt & Vasiliev (2021). They measured distances to the Galactic GCs using different procedures based on *Gaia* or HST databases and supplemented their measurements with distances provided in the literature. Unfortunately, they could not apply all their procedures to all of the Galactic GCs. In fact, we highlight that, out of the 26 VVV GCs with RR Lyrae stars from our analysis, Baumgardt & Vasiliev (2021) were able to apply all their different procedures using *Gaia* and HST data only for M 22, while for 12 GCs they apply at least one, and for the remaining 13, the GGCD distance measurements come only from the literature. As noted in Sect. 3.2, we used M 22 to recalibrate our near-infrared PLZ relations. In addition to being the only cluster in our sample for which Baumgardt & Vasiliev (2021) were able to apply all their different procedures from the *Gaia* and HST data, M 22 also contains the largest number of references in the literature. For the remaining 25 VVV GCs with RR Lyrae members for which we derived distances, ten GCs show differences between our distances and GGCD distances smaller than 5 percent, five


Fig. 3. Ratio of distances calculated using RR Lyrae stars in the VVV GCs compared to those from the GGCD, plotted against the number of RR Lyrae stars present in each GCs. Blue inverted triangles represent GCs where Baumgardt & Vasiliev (2021) were able to apply several techniques based on *Gaia* and HST data to measure distances, cyan squares indicate GCs where only one technique was used, while magenta dots show GCs lacking *Gaia* or HST measurements, relying solely on distances reported in the literature.

GCs show differences between 5 and 10 percent, and there are ten GCs for which our RR Lyrae-calculated distances are underestimated by more than 10 percent compared to those in the GGCD (see Fig. 3), with differences as severe as ~33 percent for Terzan 1. We should note, however, that this last group where the agreement is worst, primarily contains GCs for which distances in the GGCD come from literature. Conversely, most of the VVV GCs for which more than one method based on *Gaia* or HST databases was applied in Baumgardt & Vasiliev (2021) are included in the group with smaller differences. We should also highlight that most of the clusters for which only one candidate RR Lyrae star is detected are found in the group where the agreement is poorer (see Fig. 3). The fact that they have only one detected RR Lyrae star, and that the latter are located in their innermost, highly crowded regions ($r < 1.75 R_h$), renders their derived distances and extinction values more prone to systematic uncertainties affecting the RR Lyrae photometry. An alternative, of course, is that such stars do not, in fact, belong to the GCs.

7. Conclusions

We conducted a study of Galactic GCs located toward the innermost regions of the Galaxy to search for their RR Lyrae variable stars. Using the recent VIVACE and VIRAC2 catalogs, both based on VVV near-infrared observations, we explored the presence of these classical pulsators in the 41 GCs listed in the GGCD within the VVV survey footprint. To determine membership for each GC, we developed a methodology that incorporates PM, projected proximity to the cluster center, and distance moduli derived from the PLZ relations. As a by-product of this analysis, we also calculated the PM for all these VVV GCs, independently confirming *Gaia*'s measurements except for two of the most reddened GCs: UKS 1 and 2MASS-GC02.

Our study found RR Lyrae variable stars in 26 of the sampled VVV GCs. The only clusters lacking RR Lyrae stars were either metal-rich GCs or a few sparsely populated metal-poor GCs. We successfully identified most of the known RR Lyrae stars listed in the CVSGC for these GCs, missing only those located in the crowded central regions, where even PSF photometry struggles to resolve individual stellar sources. On the other hand, we were able to assign membership to RR Lyrae stars located in the outskirts of the GCs, which had not been previously considered. Our membership assignments largely align with those from recent studies in the literature for most of the RR Lyrae stars. Notably, our analysis led to the discovery of unreported RR Lyrae stars in 16 VVV GCs, including the first detection of several of these classic pulsators in the highly reddened clusters UKS 1 and VVV-CL160. We also identified one RR Lyrae star as a potential candidate in each of Terzan 4 and Terzan 9.

Building on the tight PLZ relations exhibited by RR Lyrae stars in the near-infrared, and assuming a Cardelli et al. (1989) canonical extinction law for those VVV GCs with $|l| > 5°$ and a Sanders et al. (2022) non-canonical law for those VVV GCs closer to the Galactic plane, with $|l| < 4°$, we provided distances and near-infrared color-excesses for 26 low-latitude GCs. As expected, the GCs closer to the Galactic plane were found to be the most heavily reddened. Our analysis also revealed that all but five of these GCs are located within the Galactic bulge. Five of our sampled GCs – FSR 1716, NGC 6380, NGC 6401, NGC 6558, and NGC 6642 – are even located less than 1 kpc from the Galactic center.

We compared our RR Lyrae-derived distances with those from the GGCD. We found good agreement, within the error, and typically within 5 percent, for the GCs for which the GGCD provides distances measured based on *Gaia*. However, there are ten GCs whose distances differ significantly, mostly encompassing GCs with no *Gaia* measurement. The averaged distances from the literature provided by the GGCD for the GCs in this group is usually underestimated by more than 10 percent. Most of them contain a significant number of RR Lyrae members, which provide compatible distances to support our results, even though we recommend some caution in those few cases where a cluster contains a single identified RR Lyrae member.

Data availability

Full Table D.2 is available in electronic form at the CDS via anonymous ftp to cdsarc.cds.unistra.fr (130.79.128.5) or via https://cdsarc.cds.unistra.fr/viz-bin/cat/J/A+A/695/A47

References

Alonso-García, J., Mateo, M., Sen, B., Banerjee, M., & von Braun, K. 2011, AJ, 141, 146
Alonso-García, J., Mateo, M., Sen, B., et al. 2012, AJ, 143, 70
Alonso-García, J., Dékány, I., Catelan, M., et al. 2015, AJ, 149, 99
Alonso-García, J., Minniti, D., Catelan, M., et al. 2017, ApJ, 849, L13
Alonso-García, J., Saito, R. K., Hempel, M., et al. 2018, A&A, 619, A4
Alonso-García, J., Smith, L. C., Catelan, M., et al. 2021, A&A, 651, A47
Aravena Rojas, G. 2020, Master's thesis, Universidad de Antofagasta, Chile
Arellano Ferro, A., Prudil, Z., Yepez, M. A., Bustos Fierro, I., & Luna, A. 2023, Ap&SS, 368, 91
Arellano Ferro, A., Zerpa Guillen, L. J., Yepez, M. A., et al. 2024, MNRAS, 532, 2159
Baumgardt, H., & Hilker, M. 2018, MNRAS, 478, 1520
Baumgardt, H., & Vasiliev, E. 2021, MNRAS, 505, 5957
Baumgardt, H., Hilker, M., Sollima, A., & Bellini, A. 2019, MNRAS, 482, 5138
Baumgardt, H., Hénault-Brunet, V., Dickson, N., & Sollima, A. 2023, MNRAS, 521, 3991
Belokurov, V., & Kravtsov, A. 2024, MNRAS, 528, 3198
Braga, V. F., Stetson, P. B., Bono, G., et al. 2019, A&A, 625, A1
Carballo-Bello, J. A., Ramírez Alegría, S., Borissova, J., et al. 2016, MNRAS, 462, 501
Cardelli, J. A., Clayton, G. C., & Mathis, J. S. 1989, ApJ, 345, 245
Carretta, E., Bragaglia, A., Gratton, R., D'Orazi, V., & Lucatello, S. 2009, A&A, 508, 695
Catelan, M., & Smith, H. A. 2015, Pulsating Stars (Weinheim: Wiley-VCH)
Catelan, M., Pritzl, B. J., & Smith, H. A. 2004, ApJS, 154, 633
Clement, C. M., Muzzin, A., Dufton, Q., et al. 2001, AJ, 122, 2587
Contreras Ramos, R., Minniti, D., Fernández-Trincado, J. G., et al. 2018, ApJ, 863, 78
Crociati, C., Valenti, E., Ferraro, F. R., et al. 2023, ApJ, 951, 17
Cruz Reyes, M., Anderson, R. I., Johansson, L., Netzel, H., & Medaric, Z. 2024, A&A, 684, A173
Cusano, F., Moretti, M. I., Clementini, G., et al. 2021, MNRAS, 504, 1
Dékány, I., Hajdu, G., Grebel, E. K., & Catelan, M. 2019, ApJ, 883, 58
Del Principe, M., Piersimoni, A. M., Storm, J., et al. 2006, ApJ, 652, 362
Fanelli, C., Origlia, L., Mucciarelli, A., et al. 2024, A&A, 688, A154
Fernández-Trincado, J. G., Minniti, D., Beers, T. C., et al. 2020, A&A, 643, A145
Fernández-Trincado, J. G., Minniti, D., Souza, S. O., et al. 2021, ApJ, 908, L42
Gaia Collaboration (Prusti, T., et al.) 2016, A&A, 595, A1
Garro, E. R., Minniti, D., Gómez, M., et al. 2022, A&A, 658, A120
Gonzalez, O. A., Minniti, D., Valenti, E., et al. 2018, MNRAS, 481, L130
Gran, F., Zoccali, M., Saviane, I., et al. 2022, MNRAS, 509, 4962
GRAVITY Collaboration (Abuter, R., et al.) 2021, A&A, 647, A59
Holoien, T. W. S., Marshall, P. J., & Wechsler, R. H. 2017, AJ, 153, 249
Kerber, L. O., Libralato, M., Souza, S. O., et al. 2019, MNRAS, 484, 5530
Koch, A., Kunder, A., & Wojno, J. 2017, A&A, 605, A128
Kunder, A., Prudil, Z., Covey, K. R., et al. 2024, AJ, 167, 21
Majaess, D., Turner, D., & Gieren, W. 2012a, PASP, 124, 1035
Majaess, D., Turner, D., Gieren, W., & Lane, D. 2012b, ApJ, 752, L10
Marino, A. F., Milone, A. P., Renzini, A., et al. 2019, MNRAS, 487, 3815
Massari, D., Koppelman, H. H., & Helmi, A. 2019, A&A, 630, L4
Milone, A. P., Piotto, G., Renzini, A., et al. 2017, MNRAS, 464, 3636
Minniti, D., Lucas, P. W., Emerson, J. P., et al. 2010, New Astron., 15, 433
Minniti, D., Palma, T., Dékány, I., et al. 2017, ApJ, 838, L14
Minniti, D. 2018, in The Vatican Observatory, Castel Gandolfo: 80th Anniversary Celebration, 51, eds. G. Gionti, & J.-B. Kikwaya Eluo, 63
Minniti, D., Fernández-Trincado, J. G., Gómez, M., et al. 2021, A&A, 650, L11
Molnar, T. A., Sanders, J. L., Smith, L. C., et al. 2022, MNRAS, 509, 2566
Navarrete, C., Catelan, M., Contreras Ramos, R., et al. 2017, A&A, 604, A120
Nishiyama, S., Nagata, T., Kusakabe, N., et al. 2006, ApJ, 638, 839
Nogueras-Lara, F., Gallego-Calvente, A. T., Dong, H., et al. 2018, A&A, 610, A83
Oliveira, R. A. P., Ortolani, S., Barbuy, B., et al. 2022, A&A, 657, A123
Peñaloza, F., Pessev, P., Vásquez, S., et al. 2015, PASP, 127, 329
Prieto, G., Catelan, M., Contreras Ramos, R., et al. 2012, A&A, 543, A148
Pritzl, B., Smith, H. A., Catelan, M., & Sweigart, A. V. 2000, ApJ, 530, L41
Pritzl, B. J., Smith, H. A., Stetson, P. B., et al. 2003, AJ, 126, 1381
Prudil, Z., & Arellano Ferro, A. 2024, MNRAS, 534, 3654
Saito, R. K., Hempel, M., Minniti, D., et al. 2012, A&A, 537, A107
Saito, R. K., Hempel, M., Alonso-García, J., et al. 2024, A&A, 689, A148
Sanders, J. L., Smith, L., González-Fernández, C., Lucas, P., & Minniti, D. 2022, MNRAS, 514, 2407
Schechter, P. L., Mateo, M., & Saha, A. 1993, PASP, 105, 1342
Schiavon, R. P., Phillips, S. G., Myers, N., et al. 2024, MNRAS, 528, 1393
Smith, L. C., Lucas, P. W., Kurtev, R., et al. 2018, MNRAS, 474, 1826

Smith, L. C., Lucas, P. W., Koposov, S. E., et al. 2025, MNRAS, 536, 3707
Soszyński, I., Dziembowski, W. A., Udalski, A., et al. 2011, Acta Astron., 61, 1
Soszyński, I., Udalski, A., Szymański, M. K., et al. 2014, Acta Astron., 64, 177
Soszyński, I., Udalski, A., Wrona, M., et al. 2019, Acta Astron., 69, 321
Tsapras, Y., Arellano Ferro, A., Bramich, D. M., et al. 2017, MNRAS, 465, 2489
Valenti, E., Origlia, L., & Rich, R. M. 2011, MNRAS, 414, 2690
Valenti, E., Origlia, L., Mucciarelli, A., & Rich, R. M. 2015, A&A, 574, A80
Vasiliev, E., & Baumgardt, H. 2021, MNRAS, 505, 5978
Vásquez, S., Saviane, I., Held, E. V., et al. 2018, A&A, 619, A13
Vásquez Zapata, A. F. 2021, Master's thesis, Universidad de Antofagasta, Chile
Villanova, S., Moni Bidin, C., Mauro, F., Munoz, C., & Monaco, L. 2017, MNRAS, 464, 2730

[1] Centro de Astronomía (CITEVA), Universidad de Antofagasta, Av. Angamos 601, Antofagasta, Chile

[2] Millennium Institute of Astrophysics, Nuncio Monseñor Sotero Sanz 100, Of. 104, Providencia, Santiago, Chile

[3] Institute of Astronomy, University of Cambridge, Madingley Road, Cambridge, CB3 0HA, UK

[4] Department of Physics and Astronomy, University College London, London WC1E 6BT, UK

[5] Instituto de Astrofísica, Facultad de Ciencias Exactas, Universidad Andrés Bello, Fernández Concha 700, Las Condes, Santiago, Chile

[6] Vatican Observatory, Vatican City State V-00120, Italy

[7] Instituto de Astrofísica, Facultad de Física, Pontificia Universidad Católica de Chile, Av. Vicuña Mackenna 4860, 7820436 Macul, Santiago, Chile

[8] Instituto de Física y Astronomía, Universidad de Valparaíso, Av. Gran Bretaña 1111, Playa Ancha, Casilla 5030, Chile

[9] Vera C. Rubin Observatory, AURA/NOIRLab, La Serena, Chile

[10] Instituto de Alta Investigación, Universidad de Tarapacá, Casilla 7D, Arica, Chile

[11] Instituto de Astronomía, Universidad Católica del Norte, Av. Angamos 0610, Antofagasta, Chile

[12] Instituto de Astronomía y Ciencias Planetarias, Universidad de Atacama, Copayapu 485, Copiapó, Chile

[13] ESO – European Southern Observatory, Alonso de Córdova 3107, Vitacura, Santiago, Chile

[14] Centre for Astrophysics, University of Hertfordshire, Hatfield AL10 9AB, UK

[15] Max Planck Institute for Astronomy, Königstuhl 17, 69117 Heidelberg, Germany

[16] Mount Saint Vincent University, Halifax, Canada

[17] Departamento de Física, Universidade Federal de Santa Catarina, Trindade 88040-900, Florianópolis, SC, Brazil

[18] Cerro Tololo Inter-American Observatory/NSF's NOIRLab, Casilla 603, La Serena, Chile
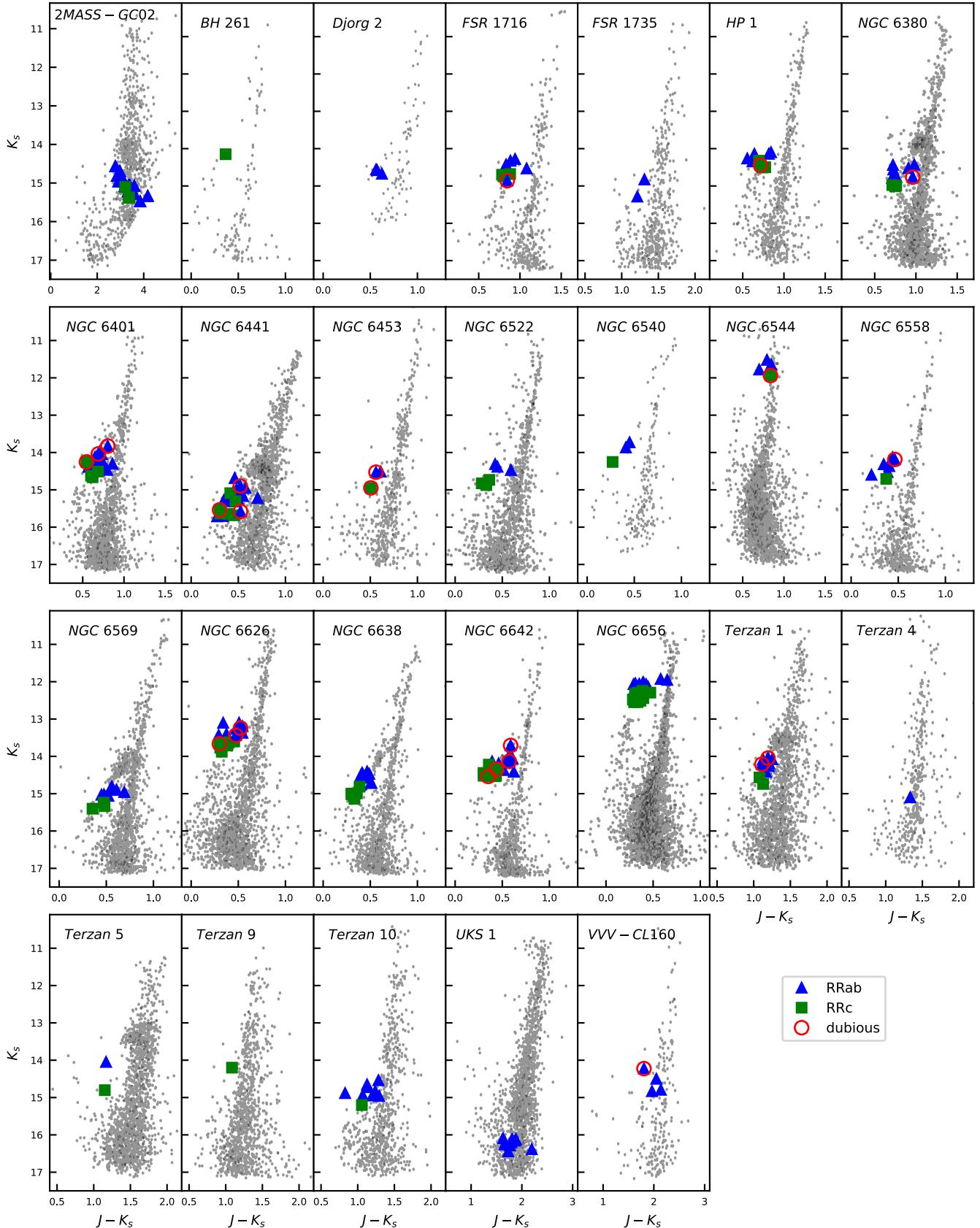
Appendix A: Positions and physical parameters of the VVV GCs

Table A.1. Positions and physical parameters of the target clusters.
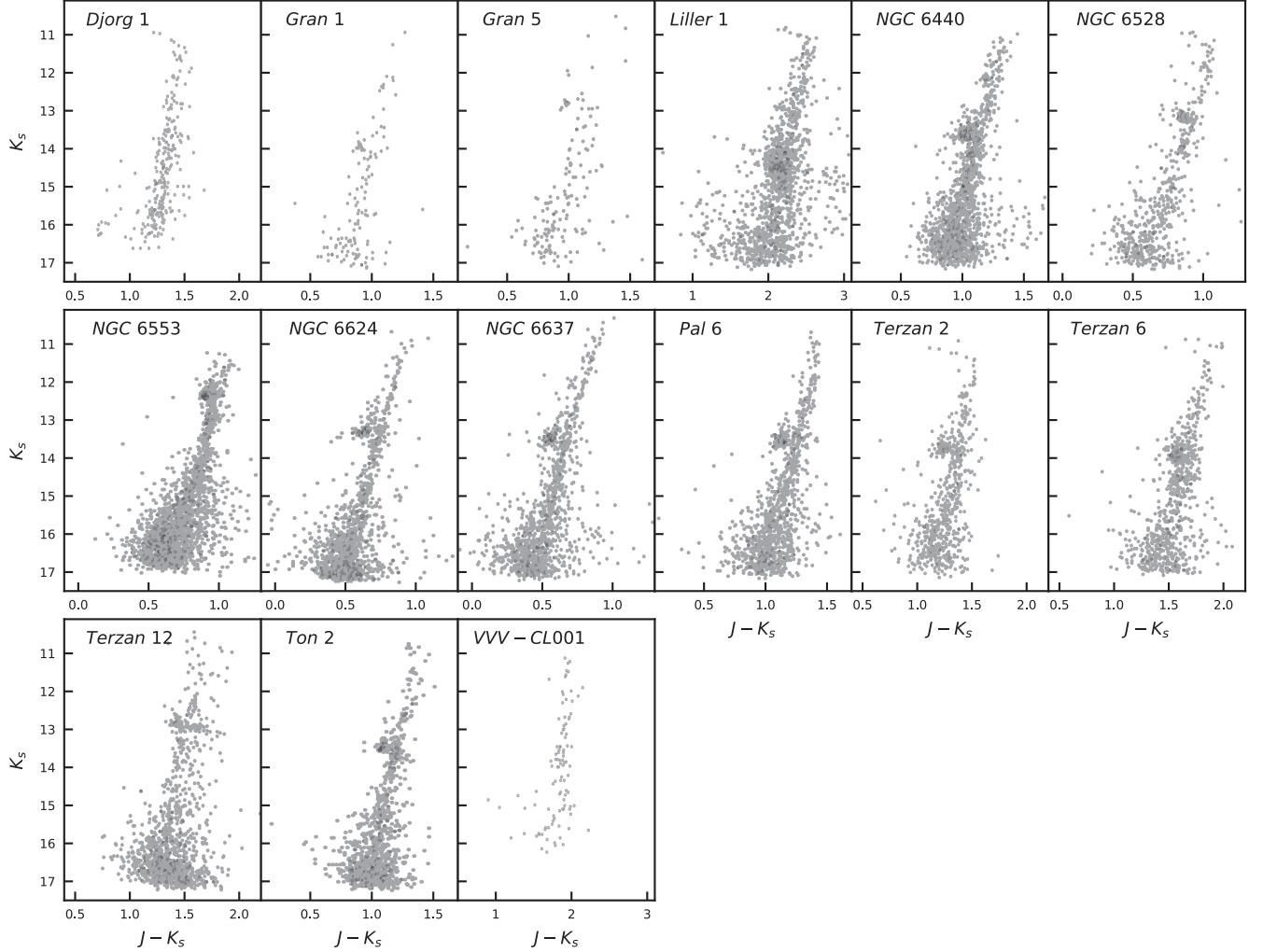
Cluster	α(J2000) (h:m:s)	δ(J2000) (d:m:s)	l (deg)	b (deg)	[Fe/H] (dex)	M_V (mag)	Mass ($\times 10^4 M_\odot$)	R_h (arcmin)	R_t (arcmin)
2MASS-GC02	18:09:36.50	-20:46:44.0	9.782	-0.615	-1.08[a]	24.6	1.56	1.39	9.81
BH 261	18:14:06.60	-28:38:06.0	3.362	-5.27	-1.1 [b]	11.26	2.38	1.65	11.59
Djorg 1	17:47:28.70	-33:03:59.0	356.675	-2.484	-1.36[c]	13.08	8.43	1.43	8.82
Djorg 2	18:01:49.05	-27:49:32.9	2.763	-2.508	-1.07[d]	10.7	13.4	1.82	6.06
FSR 1716	16:10:30.00	-53:44:56.0	329.778	-1.593	-1.38[e]	13.06	5.66	1.71	15.79
FSR 1735	16:52:10.60	-47:03:29.0	339.188	-1.853	-0.9 [f]	14.38	9.98	0.79	13.37
Gran 1	17:58:36.24	-32:01:12.0	358.767	-3.977	-1.19[g]	12.4	2.61	2.38	7.92
Gran 5	17:48:54.72	-24:10:12.0	4.459	1.839	-1.56[g]	12.11	2.29	1.21	15.06
HP 1	17:31:05.20	-29:58:54.0	357.425	2.115	-1.21[d]	11.07	13.7	1.52	9.11
Liller 1	17:33:24.56	-33:23:22.4	354.84	-0.161	-0.14[d]	15.73	101.0	0.55	16.58
NGC 6380	17:34:28.47	-39:04:10.3	350.182	-3.422	-0.78[d]	10.7	34.1	1.12	14.39
NGC 6401	17:38:36.53	-23:54:34.6	3.45	3.98	-1.09[d]	9.97	12.1	1.07	7.31
NGC 6440	17:48:52.84	-20:21:37.5	7.729	3.801	-0.53[h]	8.97	56.9	0.55	14.12
NGC 6441	17:50:13.06	-37:03:05.2	353.532	-5.006	-0.49[d]	7.12	139.0	0.58	29.25
NGC 6453	17:50:51.72	-34:35:54.5	355.718	-3.872	-1.57[c]	9.19	16.8	0.94	11.24
NGC 6522	18:03:34.07	-30:02:02.3	1.025	-3.926	-1.22[d]	8.28	21.4	1.17	7.24
NGC 6528	18:04:49.61	-30:03:20.8	1.139	-4.174	-0.16[d]	9.71	9.44	1.08	4.82
NGC 6540	18:06:08.56	-27:45:55.0	3.285	-3.313	-1.02[d]	9.74	5.62	1.54	13.21
NGC 6544	18:07:20.12	-24:59:53.6	5.837	-2.202	-1.52[d]	7.86	8.15	2.05	63.62
NGC 6553	18:09:17.52	-25:54:29.0	5.253	-3.029	-0.19[d]	8.04	22.9	1.48	30.85
NGC 6558	18:10:17.75	-31:45:52.2	0.199	-6.023	-0.99[d]	9.66	3.13	0.68	3.95
NGC 6569	18:13:38.80	-31:49:36.8	0.481	-6.681	-0.92[d]	8.9	22.9	0.85	14.01
NGC 6624	18:23:40.51	-30:21:39.7	2.788	-7.913	-0.69[i]	8.03	10.3	0.73	7.21
NGC 6626	18:24:32.89	-24:52:11.4	7.798	-5.581	-1.29[j]	6.85	27.0	1.03	30.36
NGC 6637	18:31:23.10	-32:20:53.1	1.723	-10.269	-0.59[k]	7.62	13.8	0.93	9.35
NGC 6638	18:30:56.10	-25:29:50.9	7.896	-7.153	-0.99[k]	8.79	12.4	0.65	10.21
NGC 6642	18:31:54.23	-23:28:32.2	9.815	-6.439	-1.09[d]	9.65	3.95	0.59	6.93
NGC 6656	18:36:23.94	-23:54:17.1	9.892	-7.552	-1.7 [d]	5.06	47.0	3.31	80.03
Pal 6	17:43:42.19	-26:13:30.0	2.09	1.779	-0.92[d]	11.6	8.56	1.11	5.09
Terzan 1	17:35:47.20	-30:28:54.4	357.558	0.991	-1.26[l]	12.4	19.9	0.89	23.17
Terzan 2	17:27:33.10	-30:48:08.4	356.319	2.298	-0.86[d]	13.11	8.05	1.06	5.52
Terzan 4	17:30:39.00	-31:35:43.9	356.024	1.308	-1.38[d]	13.43	18.1	1.48	7.11
Terzan 5	17:48:04.85	-24:46:44.6	3.839	1.687	-0.78[d]	12.36	109.0	0.92	26.62
Terzan 6	17:50:46.38	-31:16:31.4	358.571	-2.162	-0.65[m]	14.47	10.0	0.5	6.57
Terzan 9	18:01:38.80	-26:50:23.0	3.603	-1.989	-1.36[d]	12.73	13.7	0.99	18.83
Terzan 10	18:02:57.80	-26:04:01.0	4.421	-1.864	-1.62[d]	14.73	31.9	1.16	13.99
Terzan 12	18:12:15.80	-22:44:31.0	8.358	-2.101	-0.56[d]	13.82	3.76	1.18	16.55
Ton 2	17:36:10.08	-38:33:22.0	350.793	-3.424	-0.74[d]	11.66	4.31	1.41	10.6
UKS 1	17:54:27.19	-24:08:43.0	5.125	0.764	-1.0 [d]	17.3	7.99	0.66	10.6
VVV-CL001	17:54:42.50	-24:00:53.0	5.267	0.78	-2.45[n]	14.2	15.4	1.0	15.5
VVV-CL160	18:06:57.00	-20:00:40.0	10.151	0.302	-1.32[o]	15.6	5.28	1.66	9.87

Notes. Equatorial and Galactic coordinates, absolute integrated visual magnitudes, masses, half-light and tidal radii are taken from the GGCD. Iron contents are taken from [a]Peñaloza et al. (2015); [b]Kunder et al. (2024); [c]Vásquez et al. (2018); [d]Schiavon et al. (2024); [e]Koch et al. (2017); [f]Carballo-Bello et al. (2016); [g]Gran et al. (2022); [h]Crociati et al. (2023); [i]Valenti et al. (2011); [j]Villanova et al. (2017); [k]Carretta et al. (2009); [l]Valenti et al. (2015); [m]Fanelli et al. (2024); [n]Fernández-Trincado et al. (2021); [o]Garro et al. (in prep).

Appendix B: Near-infrared CMDs for the VVV GCs
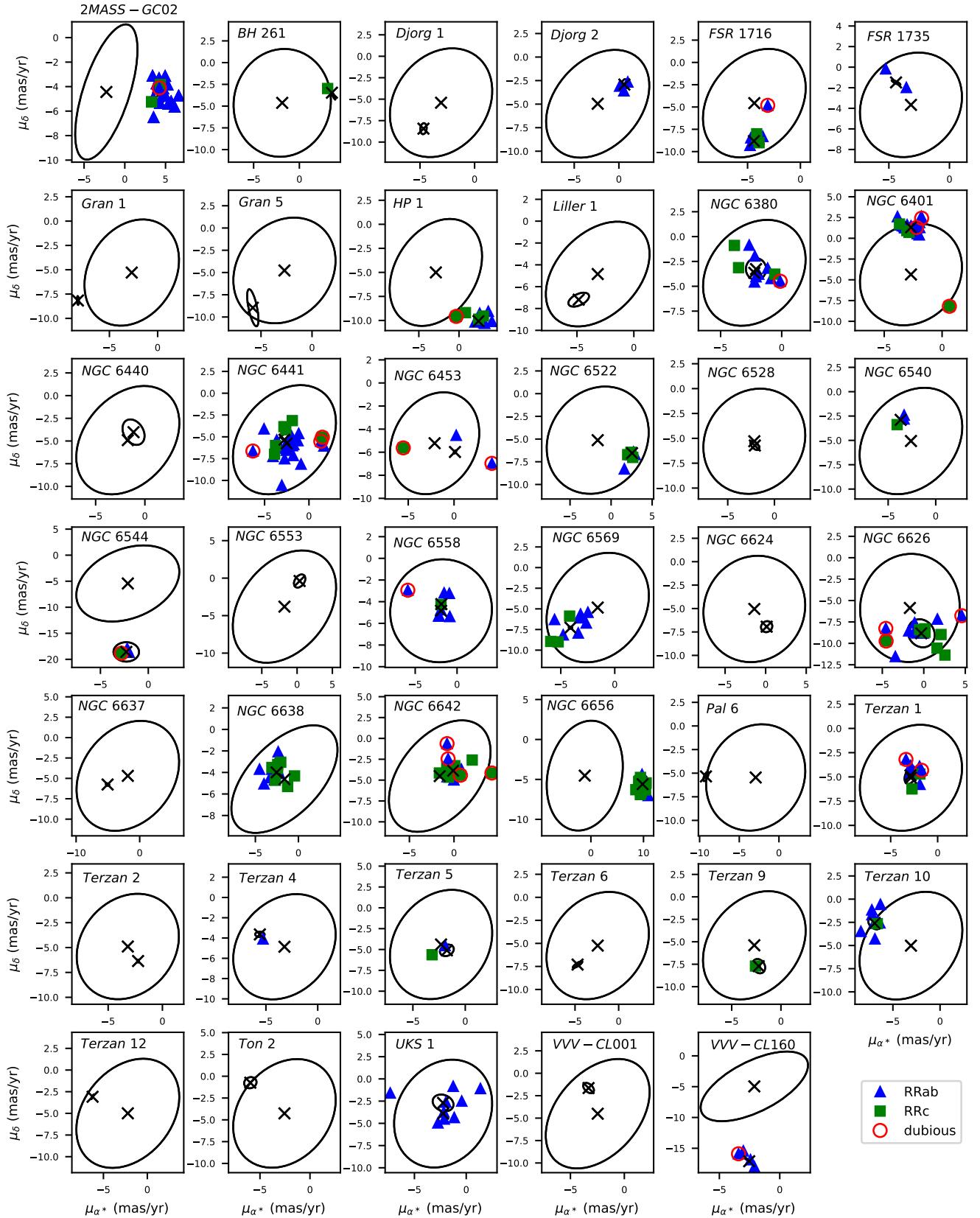
Fig. B.1. Near-infrared CMDs for the VVV GCs with assigned RR Lyrae members. The diagrams include only stars located in the innermost GC regions ($r \leq 1.0'$), selected as candidates by our PM XDGMM classifier. RR Lyrae stars for each GC are overplotted, with RRab stars represented as blue triangles and RRc stars as green squares. Dubious candidates are highlighted with red circles.

Fig. B.2. Near-infrared CMDs for the VVV GCs with no RR Lyrae members. To reduce contamination, only stars located within $r \leq 1.0'$ of the cluster centers and selected as candidates by our PM XDGMM classifier are included in the plots.

Appendix C: VPDs and PM for the VVV GCs

Fig. C.1. VPDs showing the PM of the RR Lyrae cluster members. RRab stars are represented as blue triangles, while RRc stars are shown as green squares. Red circles indicate dubious candidates. Ellipses representing the 2σ distributions of field and cluster stars, as determined by our XDGMM algorithm, are overplotted, with crosses marking the centers of both distributions.

Table C.1. Proper motions of the VVV GCs.

| Cluster	μ_{α^*} (mas yr^{-1})	μ_δ (mas yr^{-1})	$\mu_{\alpha^* GGCD}$ (mas yr^{-1})	$\mu_{\delta GGCD}$ (mas yr^{-1})
2MASS-GC 02	4.2 ± 0.4	-4.6 ± 0.4	-2.924 ± 0.22	-3.776 ± 0.174
BH 261	3.6 ± 0.2	-3.5 ± 0.4	3.589 ± 0.022	-3.57 ± 0.02
Djorg 1	-4.7 ± 0.1	-8.4 ± 0.3	-4.725 ± 0.028	-8.47 ± 0.021
Djorg 2	0.6 ± 0.2	-2.9 ± 0.3	0.72 ± 0.021	-3.003 ± 0.018
FSR 1716	-4.40 ± 0.24	-8.82 ± 0.24	-4.407 ± 0.029	-8.862 ± 0.026
FSR 1735	-4.41 ± 0.18	-1.49 ± 0.11	-4.57 ± 0.054	-1.515 ± 0.046
Gran 1	-8.27 ± 0.05	-8.16 ± 0.22	-8.044 ± 0.038	-8.049 ± 0.031
Gran 5	-5.8 ± 0.3	-9.0 ± 1.0	-5.353 ± 0.046	-9.312 ± 0.043
HP 1	2.43 ± 0.11	-10.07 ± 0.22	2.5 ± 0.028	-10.04 ± 0.027
Liller 1	-4.8 ± 0.5	-7.2 ± 0.3	-5.183 ± 0.176	-6.979 ± 0.143
NGC 6380	-2.1 ± 0.4	-3.3 ± 0.5	-2.186 ± 0.017	-3.256 ± 0.016
NGC 6401	-2.68 ± 0.18	1.32 ± 0.10	-2.762 ± 0.01	1.464 ± 0.008
NGC 6440	-1.2 ± 0.6	-4.0 ± 0.7	-1.189 ± 0.024	-4.004 ± 0.024
NGC 6441	-2.5 ± 0.5	-5.8 ± 0.5	-2.566 ± 0.02	-5.373 ± 0.02
NGC 6453	0.10 ± 0.07	-5.98 ± 0.07	0.165 ± 0.021	-5.92 ± 0.021
NGC 6522	2.55 ± 0.20	-6.55 ± 0.05	2.586 ± 0.014	-6.432 ± 0.014
NGC 6528	-2.10 ± 0.24	-5.72 ± 0.23	-2.173 ± 0.021	-5.643 ± 0.019
NGC 6540	-3.68 ± 0.04	-2.89 ± 0.10	-3.695 ± 0.019	-2.818 ± 0.018
NGC 6544	-2.3 ± 0.7	-18.6 ± 0.9	-2.269 ± 0.026	-18.61 ± 0.026
NGC 6553	0.4 ± 0.4	-0.4 ± 0.4	0.354 ± 0.013	-0.427 ± 0.013
NGC 6558	-1.87 ± 0.25	-4.22 ± 0.13	-1.752 ± 0.017	-4.167 ± 0.016
NGC 6569	-4.10 ± 0.08	-7.27 ± 0.07	-4.142 ± 0.01	-7.333 ± 0.009
NGC 6624	0.1 ± 0.3	-6.9 ± 0.3	0.127 ± 0.014	-6.956 ± 0.014
NGC 6626	-0.3 ± 0.8	-8.8 ± 0.8	-0.303 ± 0.018	-8.931 ± 0.018
NGC 6637	-5.05 ± 0.13	-5.76 ± 0.08	-5.053 ± 0.007	-5.825 ± 0.007
NGC 6638	-2.54 ± 0.12	-4.00 ± 0.06	-2.515 ± 0.011	-4.069 ± 0.01
NGC 6642	-0.1 ± 0.3	-3.9 ± 0.2	-0.175 ± 0.013	-3.9 ± 0.013
NGC 6656	9.8 ± 0.6	-5.6 ± 0.6	9.841 ± 0.009	-5.607 ± 0.009
Pal 6	-9.20 ± 0.17	-5.34 ± 0.25	-9.19 ± 0.021	-5.283 ± 0.018
Terzan 1	-2.9 ± 0.3	-4.8 ± 0.4	-2.886 ± 0.046	-4.87 ± 0.044
Terzan 2	-2.24 ± 0.04	-6.35 ± 0.07	-2.142 ± 0.03	-6.255 ± 0.027
Terzan 4	-5.58 ± 0.23	-3.64 ± 0.13	-5.364 ± 0.035	-3.674 ± 0.031
Terzan 5	-1.8 ± 0.3	-5.1 ± 0.3	-1.864 ± 0.03	-5.108 ± 0.027
Terzan 6	-4.7 ± 0.3	-7.3 ± 0.2	-4.993 ± 0.052	-7.458 ± 0.045
Terzan 9	-2.3 ± 0.3	-7.7 ± 0.4	-2.168 ± 0.031	-7.698 ± 0.029
Terzan 10	-6.9 ± 0.3	-2.6 ± 0.3	-6.806 ± 0.03	-2.595 ± 0.023
Terzan 12	-6.24 ± 0.08	-3.08 ± 0.13	-6.234 ± 0.016	-3.063 ± 0.013
Ton 2	-6.0 ± 0.3	-0.7 ± 0.3	-5.936 ± 0.02	-0.795 ± 0.019
UKS 1	-2.2 ± 0.5	-2.7 ± 0.5	-0.96 ± 0.207	-2.941 ± 0.135
VVV-CL 001	-3.3 ± 0.3	-1.6 ± 0.3	-3.394 ± 0.11	-1.71 ± 0.077
VVV-CL 160	-2.5 ± 0.3	-17.1 ± 0.4	-2.025 ± 0.133	-16.76 ± 0.104

Appendix D: RR Lyrae stars associated with the VVV GCs

Table D.1. Number of RR Lyrae stars associated with the VVV GCs.

Cluster	CVSGC[a]		Recent literature adds[b]		This work[c]		New in this work	
	RRab	RRc	RRab	RRc	RRab	RRc	RRab	RRc
2MASS-GC02	13	0	2	0	16(+1)	2	2(+1)	2
BH 261 (AL 3)	–	–	0	1	0	(1)	0	0
Djorg 2	5	2	–	–	3	0	0	0
FSR 1716 (VVV-GC05)	–	–	6	3	5	3	0	0
FSR 1735 (2MASS-GC03)	–	–	3	0	2	0	0	0
HP 1 (FSR 1781)	0	0	8	5	6	3(+1)	0	0
NGC 6380 (Ton 1)	0	0	7	3	7(+1)	3	1(+1)	0
NGC 6401	23	11	7	–	21(+2)	3(+1)	0	0
NGC 6441	47	26	2	1	20(+2)	5(+1)	2(+1)	1
NGC 6453	3	5	–	–	1(+1)	(1)	0	0
NGC 6522	5	6	0	1	4	3	1	0
NGC 6540 (Djorg 3)	2	1	–	–	2	1	1	0
NGC 6544	1	0	1	–	3	(1)	1	(1)
NGC 6558	7	3	–	–	6(+1)	1	(1)	0
NGC 6569	12	12	2	0	7	3	0	0
NGC 6626 (M 28)	10	8	1	3	8(+2)	6(+1)	0	0
NGC 6638	10	16	3	0	10	7	1	0
NGC 6642	11	6	1	2	8(+2)	8(+2)	1	1(+2)
NGC 6656 (M 22)	11	15	0	0	10	13	0	0
Terzan 1 (HP 2)	9	3	1	–	7(+2)	2	3	2
Terzan 4 (HP 4)	0	0	–	–	(1)	0	(1)	0
Terzan 5 (Terzan 11)	4	0	1	0	(1)	(1)	0	(1)
Terzan 9	0	0	–	–	0	(1)	0	(1)
Terzan 10	10	1	–	–	8	1	0	1
UKS 1 (FSR 16)	0	0	–	–	9	0	9	0
VVV-CL160	–	–	0	0	3(+1)	0	3(+1)	0

Notes. [a]RR Lyrae stars whose variability type is only suspected were included, while RR Lyrae flagged as field stars in the CVSGC were discarded. [b]References are available in the text from the different subsections in Sect. 5 [c]In parenthesis, we include those VIVACE RR Lyrae detections which cluster membership is dubious, as detailed in the different subsections in Sect. 5
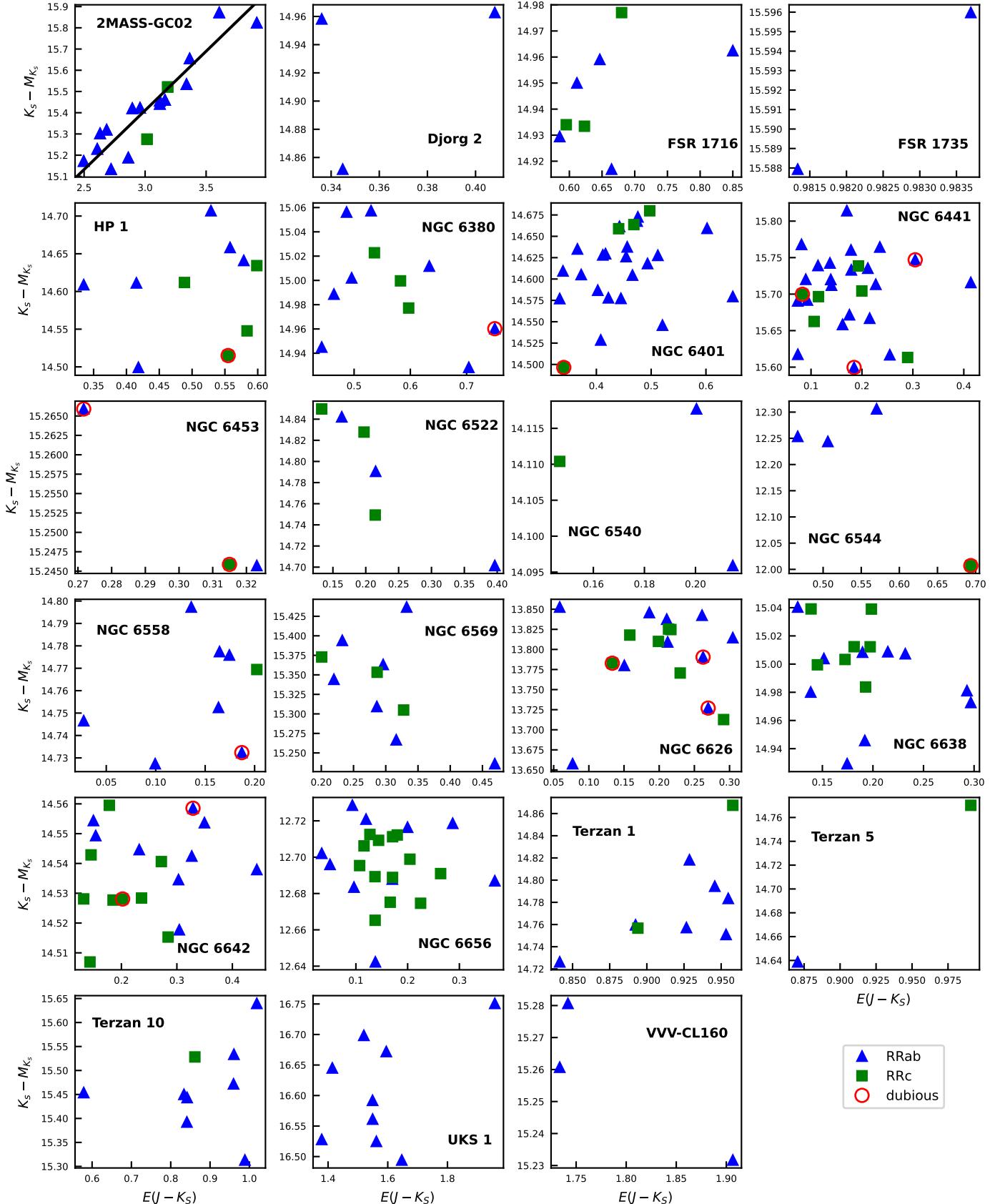
Table D.2. Observational parameters of the RR Lyrae stars associated with the VVV GCs.

Cluster	VIVACE_ID	CVSGC_ID	VIRAC2_ID	α(J2000) (deg)	δ(J2000) (deg)	Distance (arcmin)	Period (days)	K_s_amp (mag)	Z (mag)	Y (mag)	J (mag)	H (mag)	K_s (mag)	$\mu_{\alpha*}$ (mas yr^{-1})	μ_δ (mas yr^{-1})	Type	Flag[a]
2MASS-GC02	1020270	31	12715034000153	272.33583	-20.75318	4.02	0.472785	0.259	–	–	18.563 ± 0.032	16.631 ± 0.020	15.543 ± 0.003	−3.11 ± 0.95	−1.84 ± 0.89	RRab	2
2MASS-GC02	1020280	15	12719131003210	272.37179	-20.80306	2.23	0.489374	0.241	–	–	18.541 ± 0.033	16.297 ± 0.022	15.217 ± 0.003	5.00 ± 0.92	−4.77 ± 0.86	RRab	0
2MASS-GC02	1020287	–	12719131001887	272.38187	-20.79019	1.32	0.596176	0.316	–	–	17.663 ± 0.011	15.723 ± 0.015	14.694 ± 0.002	3.50 ± 0.71	−4.92 ± 0.73	RRab	0
2MASS-GC02	1020288	11	12719131009934	272.38748	-20.78549	0.91	0.551339	0.268	–	–	17.875 ± 0.015	15.950 ± 0.018	14.959 ± 0.003	3.53 ± 0.80	−6.51 ± 0.76	RRab	0
2MASS-GC02	1020289	6	12719131008099	272.39991	-20.78658	0.48	0.700046	0.334	–	18.964 ± 0.103	17.349 ± 0.011	15.582 ± 0.011	14.568 ± 0.002	4.64 ± 0.55	−4.73 ± 0.52	RRab	0
2MASS-GC02	1020295	13	12723227000289	272.40709	-20.81044	1.91	0.580317	0.221	–	18.723 ± 0.122	17.667 ± 0.011	15.812 ± 0.012	14.817 ± 0.002	4.31 ± 0.57	−5.35 ± 0.55	RRab	0
2MASS-GC02	1020300	10	12723227008013	272.41189	-20.79068	0.9	0.603299	0.279	–	–	18.114 ± 0.015	16.024 ± 0.013	14.968 ± 0.002	3.92 ± 0.52	−3.76 ± 0.50	RRab	0
2MASS-GC02	1020301	–	12719131010172	272.41044	-20.78439	0.57	0.525003	0.386	–	–	17.960 ± 0.020	16.048 ± 0.025	14.878 ± 0.004	5.68 ± 1.10	−5.22 ± 1.07	RRab	0
2MASS-GC02	1020307	12	12719131007218	272.37497	-20.76344	1.78	0.569915	0.275	–	–	19.323 ± 0.100	16.994 ± 0.030	15.478 ± 0.003	6.11 ± 1.09	−5.65 ± 1.01	RRab	0
2MASS-GC02	1020308	7	12719131007086	272.39257	-20.78226	0.57	0.651661	0.239	–	–	17.671 ± 0.016	15.773 ± 0.015	14.771 ± 0.002	4.42 ± 0.62	−4.07 ± 0.61	RRab	0
2MASS-GC02	1020309	8	12719131002646	272.39072	-20.77485	0.68	0.570445	0.268	–	–	18.466 ± 0.027	16.171 ± 0.020	15.065 ± 0.002	5.24 ± 0.79	−3.85 ± 0.75	RRab	0
2MASS-GC02	1020311	–	12719131003961	272.38034	-20.76673	1.42	0.557733	0.287	–	–	18.881 ± 0.033	16.509 ± 0.021	15.283 ± 0.003	6.61 ± 0.82	−4.74 ± 0.74	RRab	0
2MASS-GC02	1020312	–	12719131004522	272.39777	-20.76711	0.75	0.342069	0.253	–	–	18.309 ± 0.020	16.235 ± 0.020	15.103 ± 0.003	4.36 ± 0.91	−3.81 ± 0.86	RRc	0
2MASS-GC02	1020316	–	12715035003967	272.39265	-20.75689	1.42	0.333277	0.178	–	–	18.745 ± 0.030	16.548 ± 0.018	15.376 ± 0.002	3.29 ± 0.74	−5.25 ± 0.81	RRc	0
2MASS-GC02	1020325	9	12715035004265	272.41076	-20.76805	0.81	0.623703	0.208	–	–	19.511 ± 0.102	16.823 ± 0.025	15.337 ± 0.003	4.95 ± 0.91	−3.14 ± 0.84	RRab	0
2MASS-GC02	1020328	–	12715035006283	272.41191	-20.76296	1.1	0.609164	0.226	–	–	–	17.266 ± 0.033	15.542 ± 0.003	3.41 ± 1.01	−3.13 ± 0.92	RRab	0
2MASS-GC02	1020330	14	12719132005402	272.43754	-20.76922	2.07	0.608797	0.207	–	–	18.665 ± 0.023	16.336 ± 0.020	15.073 ± 0.003	5.35 ± 0.79	−5.42 ± 0.74	RRab	0
2MASS-GC02	1020332	–	12715035004061	272.41797	-20.75704	1.58	0.499091	0.160	–	–	–	16.643 ± 0.040	14.049 ± 0.001	4.24 ± 0.42	−4.10 ± 0.43	RRab	1
2MASS-GC02	1020342	18	12715035002239	272.41911	-20.73568	2.76	0.559751	0.299	–	–	18.420 ± 0.017	16.164 ± 0.013	15.065 ± 0.002	4.20 ± 0.58	−3.32 ± 0.55	RRab	0
2MASS-GC02	1020758	29	12710939000073	272.35776	-20.72830	3.92	0.540423	0.289	–	–	18.267 ± 0.015	16.243 ± 0.015	15.083 ± 0.002	4.72 ± 0.72	−4.16 ± 0.68	RRab	0
BH 261	778882	–	13501480006496	273.52074	-28.63343	0.37	0.332470	0.145	14.665 ± 0.003	14.456 ± 0.004	14.515 ± 0.004	14.216 ± 0.009	14.149 ± 0.001	3.09 ± 0.48	-2.97 ± 0.48	RRc	1
Djorg 2	784125	1	13423621019173	270.42032	-27.832249	1.85	0.515065	0.390	16.017 ± 0.010	15.600 ± 0.010	15.297 ± 0.004	14.842 ± 0.008	14.674 ± 0.001	0.99 ± 0.45	-2.65 ± 0.47	RRab	0
Djorg 2	784166	2	13423621012972	270.44548	-27.824524	0.48	0.563831	0.287	15.744 ± 0.008	15.358 ± 0.006	15.149 ± 0.003	14.706 ± 0.006	14.577 ± 0.001	0.08 ± 0.40	-3.09 ± 0.41	RRab	0
Djorg 2	786666	5	13423621012465	270.46002	-27.824954	0.3	0.517206	0.416	15.748 ± 0.012	15.299 ± 0.011	15.120 ± 0.004	14.708 ± 0.010	14.558 ± 0.001	0.55 ± 0.44	-3.59 ± 0.46	RRab	0

Notes. This table is available in its entirety in electronic form at the CDS. A portion is shown here for guidance regarding its form and content. [a]Flag 0 marks those RR Lyrae stars consider cluster bonafide members. Flag 1 marks those RR Lyrae stars whose membership is dubious. Flag 2 marks those RR Lyrae stars which appear in the CVSGC, but our analysis considers as non-members. Flag 3 marks those RR Lyrae stars with mismatch type between VIVACE and OGLE/CVSGC.

## Appendix E: Color excesses and distances to the VVV GCs

Fig. E.1. Apparent distance moduli versus color excesses for the RR Lyrae cluster members based on their near-infrared PLZ relations. RRab stars are shown as blue triangles, and RRc stars as green squares. Red circles enclose dubious candidates, which are not plotted if they exhibit large offsets. The significant differential reddening in 2MASS-GC02 leads to the high dispersion observed among its RR Lyrae members in the first panel. A solid black line shows the linear fit used to define the distance modulus and the selective-to-total extinction ratio to this GC (see Sect. 6)

Table E.1. Color excesses and distances to the VVV GCs.

Cluster	$E(Z - K_s)$ (mag)	$E(Y - K_s)$ (mag)	$E(J - K_s)$ (mag)	$E(H - K_s)$ (mag)	$R_\odot$ (kpc)	R_{GC} (kpc)	$R_{\odot,\mathrm{GGCD}}$ (kpc)	$R_{GC,\mathrm{GGCD}}$ (kpc)
2MASS-GC02	–	3.73 ± 0.21	3.04 ± 0.37	1.08 ± 0.15	6.3 ± 0.4	4.25 ± 0.07	5.50 ± 0.44	2.91 ± 0.37
BH 261	0.18 ± 0.01	0.03 ± 0.01	0.18 ± 0.01	0.01 ± 0.01	7.05 ± 0.18	3.02 ± 0.05	6.12 ± 0.26	2.20 ± 0.23
Djorg 2	0.81 ± 0.09	0.47 ± 0.09	0.36 ± 0.03	0.09 ± 0.02	9.09 ± 0.20	1.03 ± 0.17	8.76 ± 0.18	0.80 ± 0.13
FSR 1716	1.86 ± 0.13	1.19 ± 0.10	0.66 ± 0.08	0.18 ± 0.09	8.52 ± 0.10	0.54 ± 0.05	7.43 ± 0.27	4.14 ± 0.02
FSR 1735	2.74 ± 0.12	1.77 ± 0.09	0.98 ± 0.01	0.22 ± 0.03	10.72 ± 0.03	2.59 ± 0.03	9.08 ± 0.53	3.25 ± 0.22
HP 1	1.46 ± 0.07	0.94 ± 0.08	0.50 ± 0.09	0.14 ± 0.04	7.57 ± 0.18	1.52 ± 0.06	7.00 ± 0.14	1.26 ± 0.13
NGC 6380	1.51 ± 0.05	0.93 ± 0.08	0.55 ± 0.08	0.15 ± 0.06	8.99 ± 0.20	0.83 ± 0.18	9.61 ± 0.30	2.15 ± 0.21
NGC 6401	1.13 ± 0.10	0.73 ± 0.08	0.45 ± 0.07	0.13 ± 0.03	7.72 ± 0.15	0.79 ± 0.10	7.44 ± 0.22	1.03 ± 0.14
NGC 6441	0.46 ± 0.15	0.23 ± 0.13	0.16 ± 0.06	0.02 ± 0.03	13.3 ± 0.5	5.2 ± 0.5	12.73 ± 0.16	4.78 ± 0.15
NGC 6453	0.82 ± 0.01	0.53 ± 0.01	0.32 ± 0.01	0.12 ± 0.01	10.49 ± 0.08	2.36 ± 0.07	10.07 ± 0.22	2.10 ± 0.19
NGC 6522	0.58 ± 0.20	0.36 ± 0.14	0.22 ± 0.08	0.06 ± 0.06	8.7 ± 0.3	1.26 ± 0.16	7.29 ± 0.21	1.04 ± 0.17
NGC 6540	0.41 ± 0.12	0.17 ± 0.09	0.19 ± 0.03	0.00 ± 0.01	6.53 ± 0.03	1.89 ± 0.03	5.91 ± 0.27	2.34 ± 0.25
NGC 6544	1.05 ± 0.34	0.63 ± 0.20	0.51 ± 0.04	0.29 ± 0.10	2.59 ± 0.03	5.70 ± 0.03	2.58 ± 0.06	5.62 ± 0.06
NGC 6558	0.32 ± 0.13	0.13 ± 0.14	0.14 ± 0.05	0.02 ± 0.02	8.67 ± 0.16	0.73 ± 0.10	7.79 ± 0.18	0.93 ± 0.06
NGC 6569	0.63 ± 0.07	0.36 ± 0.07	0.30 ± 0.07	0.10 ± 0.06	10.7 ± 0.4	2.6 ± 0.3	10.53 ± 0.26	2.59 ± 0.23
NGC 6626	0.47 ± 0.10	0.29 ± 0.08	0.20 ± 0.07	0.03 ± 0.04	5.43 ± 0.19	2.90 ± 0.18	5.37 ± 0.10	3.02 ± 0.09
NGC 6638	0.48 ± 0.10	0.33 ± 0.09	0.19 ± 0.05	0.03 ± 0.03	9.40 ± 0.21	1.31 ± 0.19	9.78 ± 0.34	2.30 ± 0.25
NGC 6642	0.40 ± 0.14	0.25 ± 0.11	0.24 ± 0.09	0.06 ± 0.07	7.62 ± 0.19	0.92 ± 0.13	8.05 ± 0.20	1.66 ± 0.01
NGC 6656	0.34 ± 0.09	0.23 ± 0.08	0.15 ± 0.06	0.05 ± 0.08	3.30 ± 0.05	5.06 ± 0.05	3.30 ± 0.04	5.00 ± 0.03
Terzan 1	2.43 ± 0.12	1.62 ± 0.10	0.92 ± 0.04	0.31 ± 0.05	7.52 ± 0.13	1.13 ± 0.8	5.67 ± 0.17	2.52 ± 0.17
Terzan 4	2.87 ± 0.03	1.95 ± 0.03	1.14 ± 0.01	0.39 ± 0.02	9.43 ± 0.13	1.47 ± 0.10	7.59 ± 0.31	0.82 ± 0.02
Terzan 5	2.53 ± 0.22	1.59 ± 0.17	0.93 ± 0.06	0.35 ± 0.01	7.26 ± 0.11	1.55 ± 0.06	6.62 ± 0.15	1.65 ± 0.13
Terzan 9	2.19 ± 0.01	1.45 ± 0.01	0.84 ± 0.01	0.27 ± 0.01	7.36 ± 0.05	1.25 ± 0.03	5.77 ± 0.34	2.46 ± 0.33
Terzan 10	2.46 ± 0.35	1.52 ± 0.21	0.88 ± 0.12	0.30 ± 0.09	10.4 ± 0.4	2.5 ± 0.4	10.21 ± 0.40	2.17 ± 0.37
UKS 1	–	2.39 ± 0.18	1.57 ± 0.16	0.56 ± 0.09	15.4 ± 0.7	7.4 ± 0.7	15.58 ± 0.56	7.47 ± 0.54
VVV-CL 160	4.56 ± 0.12	3.13 ± 0.05	1.79 ± 0.08	0.62 ± 0.03	7.95 ± 0.12	1.79 ± 0.03	6.80 ± 0.50	1.91 ± 0.31